

PERFORMANCE ANALYSIS AND IMPROVEMENT OF SFH/DPSK IN JAMMING INTERFERENCE AND AWGN

ACCEPTED

FACULTY OF GRADUATE STUDIES

by

Qingxin Chen

B.Eng., Southeast University, China, 1989

DEAN

A Thesis Submitted in Partial Fulfillment of the
Requirements for the Degree of

MASTER OF APPLIED SCIENCE

in the Department of Electrical Engineering


We accept this thesis as conforming
to the required standard




Dr. Q. Wang, Supervisor, Dept. of Elect. & Comp. Eng.



Dr. V. K. Bhargava, Departmental Member, Dept. of Elect. & Comp. Eng.



Dr. Z. Dong, Outside Member, Dept. of Mech. Eng.



Dr. Michael Miller, External Examiner, A/Dean, Faculty of Eng.

©QINGXIN CHEN, 1992

University of Victoria

All rights reserved. Thesis may not be reproduced in whole or in part, by
photocopy or other means, without the permission of the author.

Supervisor: Dr. Qiang Wang.

Abstract

In this work, the performance of slow frequency hopped differential phase shift keying (SFH/DPSK) systems is analyzed at the block and codeword levels. The effect of error correlation in DPSK demodulation is considered when evaluating block and decoded error probabilities. The exact block and decoded error probabilities are derived and computed for additive white Gaussian noise (AWGN) and partial band noise (PBN). In the presence of tone interference and AWGN, the ranges for the block and decoded error probabilities are computed. These calculated ranges can provide a good estimate of the system performance. The effect of interleaving technique on improving the system performance is addressed under various conditions. The performance under worst case jamming is analyzed and the results are presented.

A parallel approach to the design of a universal receiver is introduced and applied to SFH/DPSK while the channel has interference from tone jamming and AWGN. It is shown that the designed receiver can always provide a decision error probability which is within a specified degradation from optimality regardless of the time-varying characteristics of the channel.

Examiners:



Dr. Q. Wang, Supervisor, Dept. of Elect. & Comp. Eng.



Dr. V. K. Bhargava, Departmental Member, Dept. of Elect. & Comp. Eng.



Dr. Z. Dong, Outside Member, Dept. of Mech. Eng.



Dr. Michael Miller, External Examiner, A/Dean, Faculty of Eng.

Contents

Abstract	ii
Contents	iv
List of Figures	xi
List of Tables	xii
Acknowledgements	xiii
Dedication	xiv
1 Introduction	1
1.1 Modulation and Interference	1
1.2 Outline of Thesis	3

2	Block and Decoded Error Probabilities of SFH/DPSK in PBN and AWGN	5
2.1	Derivation of Block Error Probability and Comparison with the Memoryless Model	5
2.2	Performance Comparison under Worst Case PBN	10
2.3	Decoded Error Probability	14
2.4	Conclusions	25
3	Block and Decoded Error Probabilities of SFH/DPSK in Tone Interference and AWGN	30
3.1	Introduction	30
3.2	Block Error Probability in Tone Interference and AWGN	31
3.3	Decoded Error Probability	38
3.4	Effect of Interleaving and Performance under Worst Case Tone Jamming	44
3.5	Conclusions	53
4	An Application of Universal Receiver Theory to SFH/DPSK with Tone Interference and AWGN	54
4.1	Introduction	54

CONTENTS

vi

4.2	Description of the Design Approach	55
4.3	Parallel Receivers for SFH/DPSK with Tone Jamming and AWGN	61
4.4	Comments	67
5	Summary and Future Work	68
5.1	Summary	68
5.2	Suggestions for Future Work	69
	Bibliography	70

List of Figures

2.1	Block error probabilities based on the memoryless model (dashdot line) and the exact expression (solid line) for BDPSK. The block length $m = 3$ and 6.	9
2.2	Block error probabilities based on the memoryless model (dashed line) and the exact expression (solid line). The block length $m = 4$ for 4-ary DPSK and $m = 2$ for 8-ary DPSK.	11
2.3	Worst case block error probabilities of BDPSK based on the memoryless model (dashdot line) and the exact expression (the upper envelope of the solid lines). The block length $m = 4$	13
2.4	An example of two adjacent blocks	14
2.5	Relationship between two block errors	15
2.6	Relationship between two adjacent code symbols	17
2.7	An example of different codeword error patterns	18

2.8 Codeword error probabilities based on the memoryless model (dashed line) and the exact expression (solid line) for BDPSK. Block length is 4 for (15, 11) RS code over $GF(2^4)$ that can correct up to two symbol errors per codeword. Block length is 5 for (31, 17) RS code over $GF(2^5)$ that can correct up to seven symbol errors per codeword. AWGN is assumed. 22

2.9 Codeword error probabilities based on the memoryless model (dashed line) and the exact expression (solid line) for 4-ary DPSK. Block length is 2. (15, 11) RS code over $GF(2^4)$ is used for correcting up to two symbol errors per codeword. AWGN is assumed. 24

2.10 Worst case codeword error probabilities based on the memoryless model (dashdot line) and the exact expression (solid line) for 4-ary DPSK. Block length is 2. (15, 7) RS code over $GF(2^4)$ is used for correcting up to four symbol errors per codeword. AWGN is assumed. 26

2.11 Worst case codeword error probabilities based on the memoryless model (dashdot line) and the exact expression (solid line) for 8-ary DPSK. Block length is 2. (63, 31) RS code over $GF(2^6)$ is used for correcting up to sixteen symbol errors per codeword. AWGN is assumed. 27

2.12 Worst case codeword error probabilities based on the memoryless model (dashdot line) and the exact expression (solid line) for BDPSK. Block length is 4. (15, 7) RS code over $GF(2^4)$ is used for correcting up to four symbol errors per codeword. AWGN is assumed. The approximate and the exact worst case error probabilities are almost equal. 28

3.1 Block error probabilities for BDPSK in both tone interference and AWGN. The block error probabilities for the all-zero block pattern (dashed line), the all-one block pattern (solid line), and the average block error probability (dash-dotted line) are shown. $m = 8$, $SNR = 8dB$ 39

3.2 The range of the decoded error probabilities for (255, 195) RS code over $GF(2^8)$ that can correct up to 30 errors. $SNR = 10dB$ 42

3.3 The range of the decoded error probabilities for (255, 223) RS code over $GF(2^8)$ that can correct up to 16 errors. $SNR = 10dB$ 43

3.4 The range of the decoded error probabilities with ideal interleaving (dash-dotted line) and without interleaving (solid line). The RS code (255, 195) over $GF(2^8)$ is used to correct up to 30 errors. $SNR = 10dB$. 45

- 3.5 The range of the decoded error probabilities with interleaving (dash-dotted line) and without interleaving (solid line). The RS code (255, 223) over $GF(2^8)$ is used to correct up to 16 errors. $SNR = 10dB$ 46
- 3.6 The decoded error probabilities with interleaving. The RS code (255, 195) is used which can correct up to 30 errors. The all-zero codeword error probability (dashed line), the average decoded error probability (dash-dotted line), and the all-one codeword error probability (solid line) are shown. $SNR = 10dB$ 47
- 3.7 The decoded error probabilities with interleaving. The RS code (255, 223) is used which can correct up to 16 errors. The all-zero codeword error probability (dashed line), the average decoded error probability (dash-dotted line), and the all-one codeword error probability (solid line) are shown. $SNR = 10dB$ 48
- 3.8 The comparison of average decoded error probabilities with interleaving. The RS codes over $GF(2^8)$ with different code rates are chosen. $SNR = 10dB$ 49
- 3.9 The average decoded error probabilities under worst case tone jamming. Ideal interleaving is applied. (255, 195) RS code over $GF(2^8)$ is used to correct up to 30 errors. $SNR = 10dB$ 51

3.10	The average decoded error probabilities under worst case tone jamming. Ideal interleaving is applied. (255,223) RS code over $GF(2^8)$ is used to correct up to 16 errors. $SNR = 10dB$	52
4.1	A parallel receiver scheme	57
4.2	The effect of ϕ_d on p_e . For dashed line, $SNR = 35dB$, $SJR = 5dB$, and $\rho = 0.5$. For solid line, $SNR = 20dB$, $SJR = 5dB$, and $\rho = 0.5$	63

List of Tables

4.1	Some typical designs for SFH/DPSK systems with tone jamming and AWGN. $SNR \in [15, 25]$, $SJR \in [10, 20]$, $\rho \in [0, 1]$	67
-----	--	----

Acknowledgements

I would like to thank my supervisor, Dr. Qiang Wang for his guidance, encouragement and patience during the course of this research, and in the preparation of this manuscript. I would also like to thank Dr. V. K. Bhargava and Mr. David Peterson for their valuable comments and criticism on both the work and the writing style.

The help and support offered by the computing personnel and secretary staff of the Department of Electrical and Computer Engineering are very appreciated. The financial support received from Dr. Qiang Wang in the form of research assistantship and from University of Victoria in the form of fellowship is gratefully acknowledged.

To my grandparents.

Chapter 1

Introduction

1.1 Modulation and Interference

We consider information transmission using differential phase shift keying (DPSK) where information is carried in phase transitions between signal vectors. DPSK is one of the most popular modulation schemes and has found applications in various communication systems. In demodulation, a *decision* is made on the phase difference between two adjacent signal vectors [1]. This detection scheme may introduce correlation in errors of two successive decisions due to the fact that there is a common received vector used in making two successive decisions. If we are only concerned with the error probability of one symbol, e.g. for an uncoded system, the error correlation is not important. However, if we are interested in a *coded system*, where an error correction code is employed, the correlation in errors will affect the performance of error correction coding and should be taken into account.

In a coded system, each *code symbol* at the decoder corresponds to a *block*, which

is defined as a group of successive DPSK decisions at the output of the demodulator. Since the last decision of a block is correlated with the first decision of the next block, block errors or code symbol errors are also correlated. This will affect the decoded error probability.

The topic of error correlation in DPSK systems received attention in the literature published in the early 1960's. Salz and Saltzberg [2], and Oberst and Schilling [3] evaluated the double symbol error probability for binary DPSK in the additive white Gaussian noise (AWGN) channel. Goldman analyzed the multiple symbol error probability for both coherent and differentially coherent M -ary PSK systems in cochannel interference plus AWGN channel [4]. The major contribution of this thesis is to extend their results to the block and codeword error probabilities analytically and evaluates the performance in the interference of partial band noise (PBN) or tone jamming combined with AWGN.

The reason for our interest in PBN and tone jamming is that we are concerned with the anti-jam performance of slow frequency hopped DPSK (SFH/DPSK) [5]. SFH/DPSK is a very important frequency-hop communication scheme and has been considered as a future Canadian military satellite communication system [6]. In SFH/DPSK spread spectrum communications, the carrier frequency varies from hop to hop. During each hop, there are multiple DPSK modulation symbols. PBN is a very common jamming model in which only a fraction ρ of the entire frequency band is jammed by AWGN with an increased one-sided power spectrum density N_J/ρ , where N_J is the effective jamming power spectral density defined as the total jamming power divided by the total spread spectrum bandwidth. The worst case PBN is such that ρ is chosen to maximize the error probabilities of concern. Jamming tone is a continuous sinusoidal wave with its initial phase uniformly distributed over

an interval of length 2π . It is an effective type of jamming because it is easy to generate, and yet hard to be eliminated by conventional noise filter due to its narrowest bandwidth. When the total jamming power is fixed, the probability ρ for each hop to be jammed can be chosen to maximize error probabilities, which is the worst case tone jamming.

In the jamming environment, the channel characteristics are uncertain to the receiver in that the jammer changes its strategies constantly to worsen the communication quality. This makes it impossible to design a receiver which performs optimally no matter what jamming strategy is being used. Specifically, in the presence of tone jamming, the structure of optimal decision regions for DPSK demodulation varies with the jamming probability ρ , corresponding signal-to-noise ratio SNR , and the signal-to-jamming ratio SJR . In this thesis, a parallel approach is introduced and applied to the design of a universal receiver which can provide nearly optimal decision error performance for SFH/DPSK systems in the interference of combined tone jamming and AWGN.

1.2 Outline of Thesis

An outline of the remainder of this thesis is as follows:

Chapter 2 and 3 concentrate on the performance analysis of SFH/DPSK systems under various interference. The interference of concern in Chapter 2 is PBN and AWGN, while in Chapter 3, tone jamming and AWGN are considered. In both chapters, the block error probabilities and decoded error probabilities are derived and computed with error correlation in DPSK demodulation considered. The effectiveness of interleaving technique is addressed. The performance under worst case

jamming is presented.

In Chapter 4, we introduce a parallel approach to the design of a type of universal receivers. The application of this approach to SFH/DPSK systems with tone interference and AWGN is explored. The performance of interest is decision error probability.

Chapter 5 summarizes this thesis and discusses several issues for further study.

Chapter 2

Block and Decoded Error Probabilities of SFH/DPSK in PBN and AWGN

2.1 Derivation of Block Error Probability and Comparison with the Memoryless Model

Let m denote the *block length* which is the number of DPSK decisions in a block, p_e be the decision error probability, and p_E be the block error probability. A block is in error if, and only if, there is at least one decision in the block in error. The often used simple memoryless model in which decision errors are considered to occur independently will result in

$$p_E = 1 - (1 - p_e)^m. \quad (2.1)$$

However, when the error correlation in DPSK demodulation is considered, the expression for the block error probability is different. For ease of understanding and to make this chapter self-contained, results for binary DPSK (BDPSK) are first given. Some of these relatively simple results for BDPSK cannot be directly

generalized to M -ary DPSK with $M > 2$.

After being disturbed by AWGN, the received signal vector will have a phase error ϕ relative to the transmitted vector. The probability density function (pdf) of ϕ is[3]

$$f(\phi) = \frac{1}{2\pi}e^{-R} + \frac{1}{2}\sqrt{\frac{R}{\pi}}e^{-R\sin^2\phi}\cos\phi[1 + \operatorname{erf}(\sqrt{R}\cos\phi)],$$

$$\phi \in [-\pi, \pi), \quad (2.2)$$

where R is the signal-to-noise ratio (SNR) which equals E_s/N_0 . Here E_s is the energy of each signal vector, and N_0 is one-sided AWGN power spectral density.

For BDPSK, the probability of error for the j th decision conditioned on the phase error in the j th received signal vector being equal to ϕ is[3]

$$p_{e_j|\phi} = \frac{1}{2}\operatorname{erfc}(\sqrt{R}\cos\phi). \quad (2.3)$$

The joint probability for double errors is

$$p_{e_{j+1},e_j} = \int_{-\pi}^{\pi} p_{e_j|\phi}^2 f(\phi) d\phi$$

$$= \int_{-\pi}^{\pi} \frac{1}{4} \operatorname{erfc}^2(\sqrt{R}\cos\phi) \left\{ \frac{1}{2\pi} e^{-R} + \frac{1}{2} \sqrt{\frac{R}{\pi}} e^{-R\sin^2\phi} \cos\phi [1 + \operatorname{erf}(\sqrt{R}\cos\phi)] \right\} d\phi. \quad (2.4)$$

Note that nonadjacent decision errors are mutually independent. That is,

$$p_{e_{j+2}|e_j} = p_{e_j} = p_{e_{j+2}} = \frac{1}{2}e^{-R}. \quad (2.5)$$

From (2.4) and (2.5), the probability for $(j+1)$ th decision to be in error conditioned on the previous decision being in error is therefore

$$p_{e_{j+1}|e_j} = \frac{p_{e_{j+1},e_j}}{p_{e_j}}. \quad (2.6)$$

Since a block is wrong if any of its decisions are wrong, the probability for a block to be correct can be written as

$$p_C = p_c p_{c|c}^{m-1}, \quad (2.7)$$

where C and c denote a correct block and a correct decision, respectively. Since the error probability of each block symbol does not depend on the specific symbol transmitted (which is not true in the next chapter, where tone jamming is present), the subscripts indicating the order of decisions are omitted for simplicity. Obviously, $p_c = 1 - p_e$, $p_{c|c}$ is derived below.

Employing Eq. (2.3), the probability for a correct decision conditioned on the phase error in the j th received vector being equal to ϕ is

$$p_{c|\phi} = 1 - \frac{1}{2} \operatorname{erfc}(\sqrt{R} \cos \phi). \quad (2.8)$$

The probability for the occurrence of two adjacent correct decisions is

$$p_{cc|\phi} = [1 - \frac{1}{2} \operatorname{erfc}(\sqrt{R} \cos \phi)]^2. \quad (2.9)$$

Averaging (2.9) over the pdf in (2.2) yields the following probability for double correct decisions

$$p_{cc} = \int_{-\pi}^{\pi} p_{cc|\phi} f(\phi) d\phi,$$

$$\begin{aligned}
&= \int_{-\pi}^{\pi} \left[1 - \frac{1}{2} \operatorname{erfc}(\sqrt{R} \cos \phi)\right]^2 \left\{ \frac{1}{2\pi} e^{-R} + \frac{1}{2} \sqrt{\frac{R}{\pi}} e^{-R \sin^2 \phi} \right. \\
&\quad \left. \cos \phi [1 + \operatorname{erf}(\sqrt{R} \cos \phi)] \right\} d\phi. \tag{2.10}
\end{aligned}$$

Then the conditional probability is $p_{c|c} = p_{cc}/p_c$, and the final result of block error probability is

$$\begin{aligned}
p_E &= 1 - p_c p_{c|c}^{m-1}, \\
&= 1 - \left(1 - \frac{1}{2} e^{-R}\right) \left\{ \frac{\int_{-\pi}^{\pi} \left[1 - \frac{1}{2} \operatorname{erfc}(\sqrt{R} \cos \phi)\right]^2 f(\phi) d\phi}{1 - \frac{1}{2} e^{-R}} \right\}^{m-1}. \tag{2.11}
\end{aligned}$$

The performance difference has been evaluated based on the memoryless model as shown in Eq. (2.1) and on the exact expression in Eq. (2.11). The exact block error probability is always lower than what the memoryless model predicts. Figure 2.1 shows results for $m = 3$ and 6. The difference in E_s/N_0 depends on the error probability of interest and decreases as the error probability decreases. It, however, has little dependence on m . For a reasonably low error probability, the inherent error correlation of DPSK can be seen to be quite weak in the wide band AWGN as far as the block error probability is concerned. The results based on the memoryless model are almost the same as the exact block error probabilities.

For M -ary DPSK, the probability of error for the j th decision conditioned on the phase error in the j th vector being ϕ is given by

$$p_{\epsilon|\phi} = \int_{\frac{\pi}{M} + \phi}^{2\pi - \frac{\pi}{M} + \phi} f(x) dx, \tag{2.12}$$

where function f is given in Eq. (2.2).

The probability for a decision error is

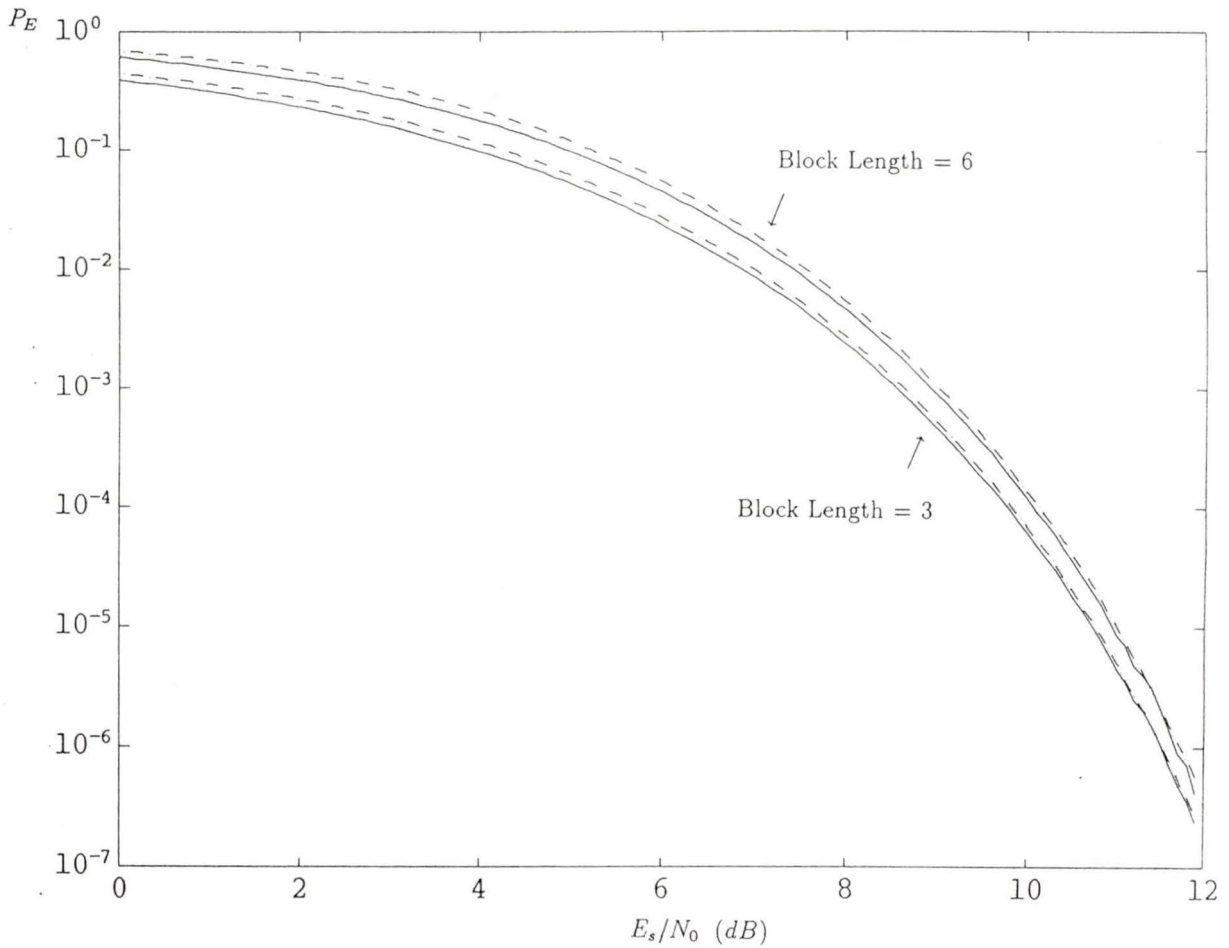


Figure 2.1: Block error probabilities based on the memoryless model (dashdot line) and the exact expression (solid line) for BDPSK. The block length $m = 3$ and 6.

$$p_e = \int_{-\pi}^{\pi} p_{e|\phi} f(\phi) d\phi. \quad (2.13)$$

The above derivation of p_e is quite straightforward, but it requires two dimensional integration. There is a computationally more efficient formula for p_e in [7] where only one integration is needed. This formula is going to be used in the next chapter for calculating the decision error probability conditioned on its being jammed by a tone with a fixed initial phase.

The probability for two adjacent decision errors is

$$p_{ee} = \int_{-\pi}^{\pi} p_{e|\phi}^2 f(\phi) d\phi, \quad (2.14)$$

and

$$p_{cc} = \int_{-\pi}^{\pi} (1 - p_{e|\phi})^2 f(\phi) d\phi. \quad (2.15)$$

The block error probability for M -ary DPSK can then be easily obtained by using some of the expressions given earlier.

Figure 2.2 shows results for 4-ary DPSK and 8-ary DPSK. From this figure, we can see that for nonbinary DPSK, the approximate block error probability based on the memoryless model is almost equal to the exact block error probability. In other words, the memoryless model is accurate in computing the block error probability.

2.2 Performance Comparison under Worst Case PBN

As mentioned earlier, the partial band noise (PBN) jamming with which a fraction ρ of the entire communication frequency band is jammed by AWGN is of interest

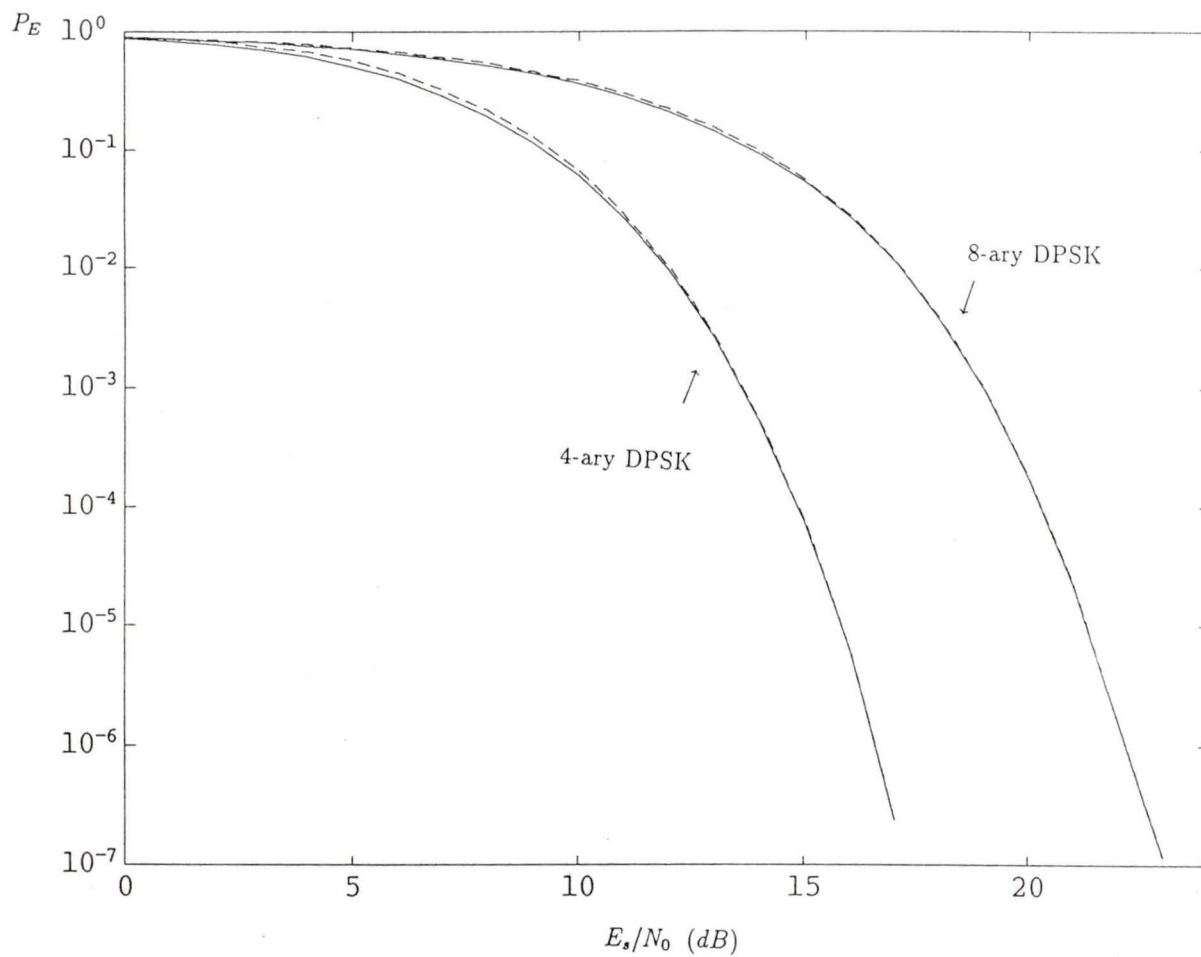


Figure 2.2: Block error probabilities based on the memoryless model (dashed line) and the exact expression (solid line). The block length $m = 4$ for 4-ary DPSK and $m = 2$ for 8-ary DPSK.

when applying DPSK to slow frequency-hop communications. In a SFH/DPSK system, the state for each hop being jammed or not is independent from one hop to another. Recall that N_J is the one-sided power spectral density of a full-band jammer. We assume that the PBN is dominant so that the effect of background noise can be ignored. The expression for block error probability can be rewritten as

$$p'_E(E_s/N_J) = \rho \times p_E\left(\frac{E_s}{N_J/\rho}\right). \quad (2.16)$$

Applying Eq. (2.16) by replacing every R in the previous results for AWGN by $\rho E_s/N_J$ and multiplying ρ to the conditional error probabilities, conditioned on being jammed, we can obtain exact block error probabilities and approximate block error probabilities based on the memoryless model in PBN. By varying ρ and plotting the curves of block error probabilities versus E_s/N_J , we can find the worst case error probabilities as the upper envelope of these curves. Figure 2.3 shows the worst case block error probabilities for the block length $m = 4$ and BDPSK. Again, the exact error probabilities are found to be lower than the approximate error probabilities based on the memoryless channel model. But the difference in E_s/N_J for a given value of error probability is about 0.5 dB which is larger than that in the presence of broad band AWGN. This increase in the difference is due to the fact that the worst case PBN jamming is always trying to take advantage of the slow varying part of the error probability curve just before it drops sharply. Over this part, the difference between the exact and the approximate block error probabilities is more appreciable than elsewhere. Note that the worst case block error probability curves are inversely linear instead of being water fall curves as the case where ρ is fixed.

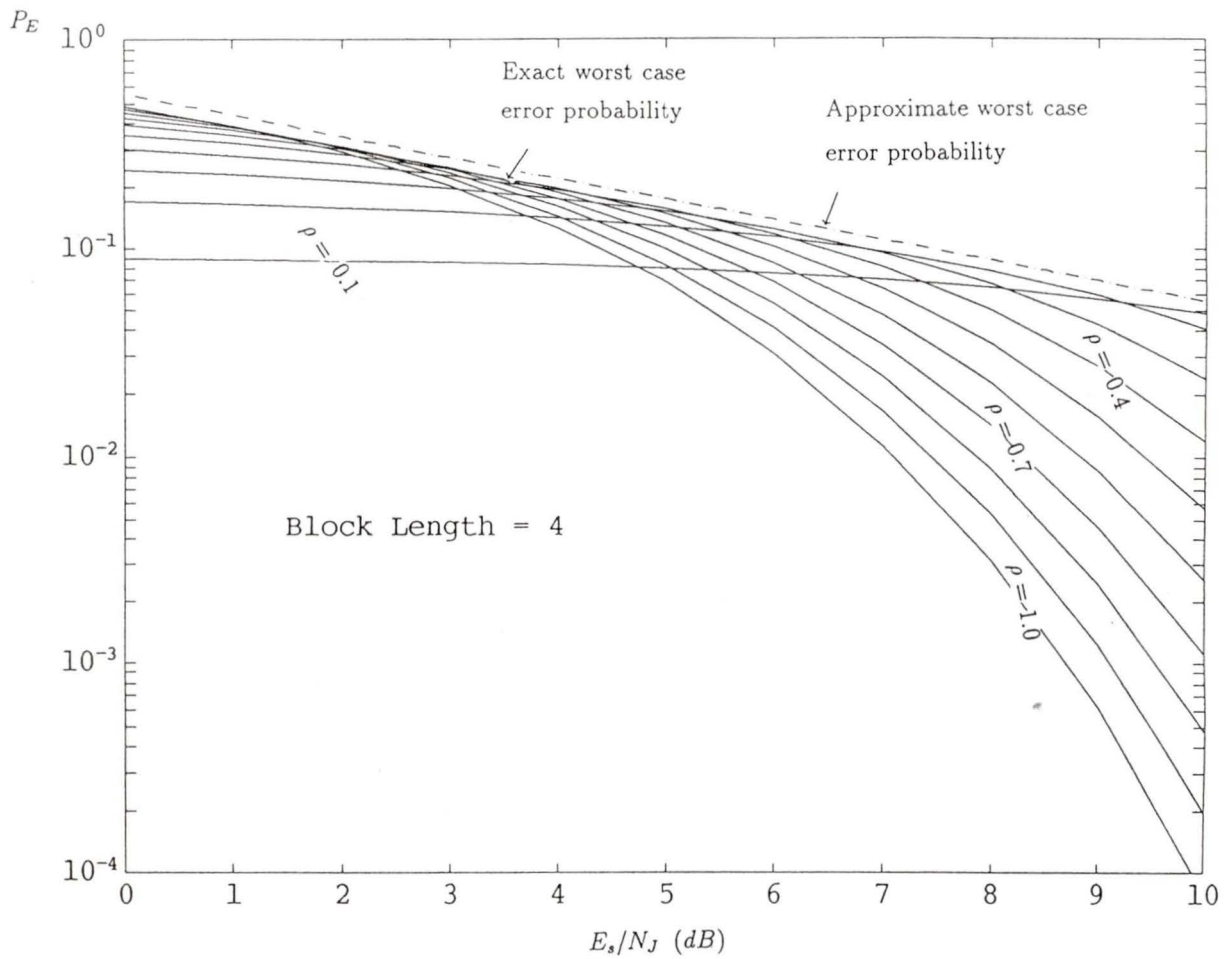


Figure 2.3: Worst case block error probabilities of BDPSK based on the memoryless model (dashdot line) and the exact expression (the upper envelope of the solid lines). The block length $m = 4$.

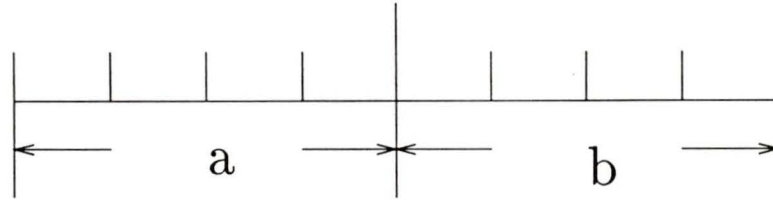


Figure 2.4: An example of two adjacent blocks

2.3 Decoded Error Probability

Suppose that a t -error correction code has length N . Then the *bounded distance decoding failure* will occur if more than t errors appear in a received codeword.

If code symbol errors are considered to occur independently, the codeword error probability or decoded error probability (i.e. decoding failure probability) is given by

$$P = \sum_{i=t+1}^N \binom{N}{i} p_E^i (1 - p_E)^{N-i}. \quad (2.17)$$

Before considering the exact decoded error probability with DPSK decision error correlation taken into account, we first look at the relationship between two adjacent blocks.

Consider the example shown in Figure 2.4. ‘a’ and ‘b’ are two adjacent blocks each consisting of four decisions. Since the last decision in block ‘a’ is correlated with the first decision in block ‘b’, these two blocks are correlated. As a preparation for the further derivation, the definitions of a number of notations are listed below.

e_a - The last decision of block ‘a’ being incorrect.

c_a - The last decision of block ‘a’ being correct.

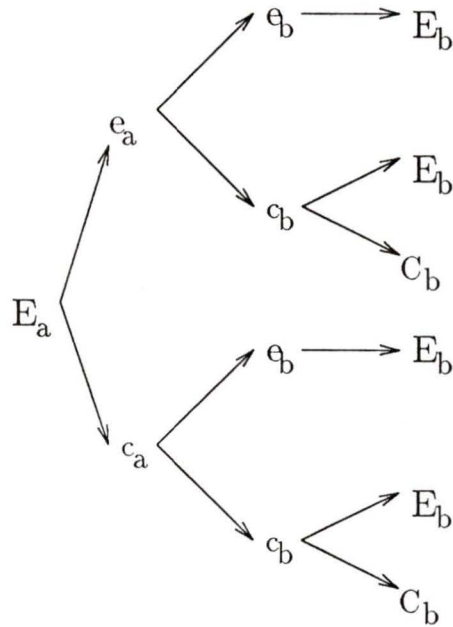


Figure 2.5: Relationship between two block errors

e_b - The first decision of block 'b' being incorrect.

c_b - The first decision of block 'b' being correct.

E_a - Block 'a' being in error.

C_a - Block 'a' being correct.

E_b - Block 'b' being in error.

C_b - Block 'b' being correct.

The tree shown in Figure 2.5 describes the correlation between two block errors under the condition that block 'a' is wrong.

We can find the conditional probability for two block errors by considering all possible paths that lead to E_b .

$$\begin{aligned}
p_{E_b|E_a} &= p_{e_a|E_a} \times p_{e_b|e_a} \times p_{E_b|e_b} \\
&\quad + p_{e_a|E_a} \times p_{c_b|e_a} \times p_{E_b|c_b} \\
&\quad + p_{c_a|E_a} \times p_{e_b|c_a} \times p_{E_b|e_b} \\
&\quad + p_{c_a|E_a} \times p_{c_b|c_a} \times p_{E_b|c_b}.
\end{aligned} \tag{2.18}$$

The conditional probabilities on the right side of Eq. (2.18) are derived as follows.

$$\begin{aligned}
p_{e_b|E_b} &= p_{e_a|E_a} = \frac{p_{E_a e_a}}{p_{E_a}} = \frac{p_{E_a|e_a} p_{e_a}}{p_{E_a}} = \frac{p_{e_a}}{p_{E_a}}, \\
p_{c_a|E_a} &= 1 - p_{e_a|E_a}, \\
p_{E_b|e_b} &= 1, \\
p_{E_b|c_b} &= \frac{p_{E_b c_b}}{1 - p_{e_b}} = \frac{(1 - p_{e_b|E_b}) p_{E_b}}{1 - p_{e_b}}, \\
p_{e_b|e_a} &= \frac{p_{e_a e_b}}{p_{e_a}}, \\
p_{c_b|e_a} &= 1 - p_{e_b|e_a}, \\
p_{e_b|c_a} &= p_{c_a|e_b} \times \frac{p_{e_b}}{p_{c_a}} = p_{c_b|e_a} \times \frac{p_{e_b}}{p_{c_a}}, \\
p_{c_b|c_a} &= 1 - p_{e_b|c_a}.
\end{aligned} \tag{2.19}$$

Since every decision has the same error probability, and so does every block, we omit the subscripts ‘ a ’ and ‘ b ’ below for convenience.

Substituting the results of Eq. (2.19) into Eq. (2.18), the block error probability conditioned on the error of the previous one is

$$\begin{aligned}
p_{E|E} &= \frac{p_{ee}}{p_E} + 2 \times \frac{(p_E - p_e)(p_e - p_{ee})}{p_E(1 - p_e)} \\
&\quad + \frac{(p_E - p_e)^2(1 - 2p_e + p_{ee})}{p_E(1 - p_e)^2}.
\end{aligned} \tag{2.20}$$

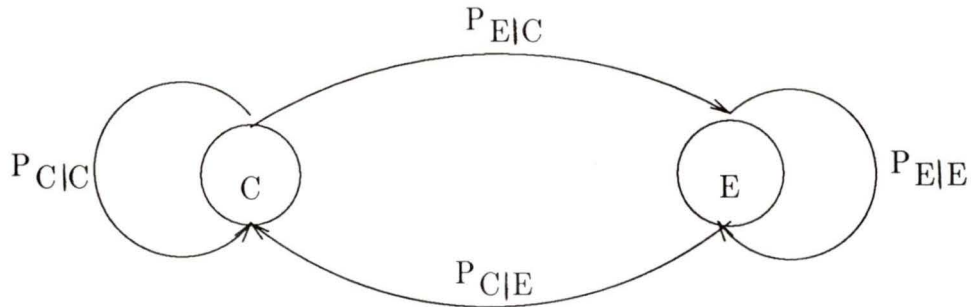


Figure 2.6: Relationship between two adjacent code symbols

With $p_{E|E}$ known, other conditional probabilities are easy to find.

$$p_{C|E} = 1 - p_{E|E}, \quad (2.21)$$

$$p_{C|C} = 1 - p_{E|C} = 1 - \frac{p_{EC}}{p_C} = 1 - \frac{p_{C|E}p_{E|C}}{p_C}, \quad (2.22)$$

$$p_{E|C} = 1 - p_{C|C}. \quad (2.23)$$

We now start the derivation of decoded error probability [9].

Figure 2.6 describes the probability relation between the performance of two adjacent code symbols. It shows that each code sequence behaves like a two-state Markov chain. If we refer to the error distribution in a codeword as an *error pattern*, different error patterns may occur with different probabilities even if the number of errors in each pattern is the same. One example is shown in Figure 2.7, where ‘1’ indicates a code symbol error, and ‘0’ indicates a correct code symbol. Although the number of errors in codeword (a) is the same as in (b), the error event probabilities P_a and P_b which are given below are different due to different error distributions.

$$P_a = p(C)p(E|C)p(E|E)p(C|E)p(E|C)p(E|E)p(C|E)p(C|C)^3,$$

0	1	1	0	1	1	0	0	0	0
---	---	---	---	---	---	---	---	---	---

(a)

0	1	0	0	0	1	0	0	1	1
---	---	---	---	---	---	---	---	---	---

(b)

Figure 2.7: An example of different codeword error patterns

$$= p(C)p(E|C)^2p(E|E)^2p(C|E)^2p(C|C)^3.$$

$$P_b = p(C)p(E|C)p(C|E)p(C|C)^2p(E|C)p(C|E)p(C|C)p(E|C)p(E|E),$$

$$= p(C)p(E|C)^3p(C|E)^2p(C|C)^3p(E|E).$$

Before proceeding to further derivation, three functions are defined as follows.

$G(k)$ – The conditional probability for one symbol error followed by k correct symbols.

$R(m, n)$ – Given that the first symbol in an n -symbol sequence is in error, the conditional probability for the occurrence of $(m - 1)$ errors in the remaining $(n - 1)$ symbols.

$p(n, m)$ – The probability for the occurrence of m errors in an n -symbol sequence.

By the definition

$$G(k) = p_{C|E} \times p_{C|C}^{k-1}, \quad k = 1, 2, \dots, \quad (2.24)$$

and for the consistency of expressions, we define

$$G(0) = 1,$$

$$R(1, 1) = 1.$$

When $m = 1$, $R(1, n)$ means that only one error happens in the first symbol of an n -symbol sequence. It is given by

$$R(1, n) = p_{C^{n-1}|E} = G(n-1), \quad n \geq 1. \quad (2.25)$$

In an n -symbol sequence, given the first symbol is incorrect, the probability for any one of the rest $(n-1)$ symbols to be incorrect is given by

$$\begin{aligned} R(2, n) &= p_{E|E}R(1, n-1) + p_{E|C}p_{C|E}R(1, n-2) + p_{E|C}p_{C^2|E}R(1, n-3) \\ &\quad + \dots + p_{E|C}p_{C^{n-2}|E}R(1, 1), \\ &= p_{E|E}R(1, n-1) + p_{E|C} \sum_{i=2}^{n-1} G(i-1)R(1, n-i), \\ &\quad 2 < n. \end{aligned} \quad (2.26)$$

From Eq. (2.26), we can obtain a recursive expression for $R(m, n)$ as follows

$$\begin{aligned} R(m, n) &= p_{E|E}R(m-1, n-1) + p_{E|C} \sum_{i=2}^{n-m+1} G(i-1)R(m-1, n-i), \\ &\quad 2 \leq m < n. \end{aligned} \quad (2.27)$$

In the case that $m = n$, the expression for $R(m, n)$ is

$$R(n, n) = p_{E|E}^{n-1}. \quad (2.28)$$

We now consider $p(n, m)$, which is the probability that m symbols in an n -symbol sequence are in error. We first partition the event that m out of n symbols are in error into two mutually exclusive events: m symbols *including* the first symbol in the n -symbol sequence are in error and m symbols *excluding* the first symbol are in error. For the second case, we can apply similar binary partition with respect to whether the second symbol is in error or not. Performing this partition repeatedly, we then have

$$\begin{aligned}
p(n, m) &= \text{Prob}\{m \text{ symbols including the first symbol are in error}\} \\
&\quad + \text{Prob}\{m \text{ symbols excluding the first symbol are in error}\} \\
&= p_E R(m, n) + \text{Prob}\{m \text{ symbols excluding the first symbol are in error}\} \\
&= p_E R(m, n) \\
&\quad + \text{Prob}\{m \text{ symbols excluding the first symbol} \\
&\quad\quad \text{but including the second symbol are in error}\} \\
&\quad + \text{Prob}\{m \text{ symbols excluding the first two symbols are in error}\} \\
&= p_E R(m, n) + p_{E|P_C|E} R(m, n - 1) \\
&\quad + \text{Prob}\{m \text{ symbols excluding the first two symbols are in error}\} \\
&= p_E G(0) R(m, n) + p_E G(1) R(m, n - 1) \\
&\quad + \text{Prob}\{m \text{ symbols excluding the first two symbols are in error}\} \\
&= \dots \\
&\quad \dots \\
&= p_E \sum_{i=1}^{n-m+1} G(i-1) R(m, n - i + 1). \tag{2.29}
\end{aligned}$$

Eq. (2.29) gives the probability for m errors occurring in an n -symbol sequence. When the n -symbol sequence is a codeword of length N , and t is the number of

correctable errors, the codeword error probability (decoded error probability) is

$$P = \sum_{i=t+1}^N p(N, i). \quad (2.30)$$

Now we have two formulas, equations (2.17) and (2.30), for calculating codeword error probability. One is for the approximate error probability based on the memoryless model, and the other is for the exact error probability. Figure 2.8 shows the results obtained from these two formulas using BDPSK and (15, 11) 16-ary Reed-Solomon (RS) code and (31, 17) 32-ary RS code, respectively. The (15, 11) code has the number of correctable errors $t = 2$ and the (31, 17) code has $t = 7$. From these figures, we can see that when the error probability is very high, the approximate error probability is almost equal to the exact error probability. When the error probability is reasonably low, however, the approximate error probability is smaller than the exact error probability. The difference increases as the error probability decreases. For a given error probability, the difference is larger for a less powerful code (e.g. (15, 11) code) or a higher rate (lower redundancy) code than for a more powerful code (e.g. (31, 17) code). This is due to the fact that the decision error correlation in DPSK causes the code symbol errors to be *bursty* which may increase the chance to have more than t errors in a codeword causing the failure of a *random* t -error correction code. The smaller the t , the more easily this happens.

Interleaving is a technique for re-ordering code symbols before their transmission. In this thesis, we restrict ourselves to block interleaving, wherein codewords are arranged in i columns of a rectangular array and then to be transmitted by column. At the receiver, the order of the code symbols is recovered by deinterleaving. i is referred to as the *interleaving span*, and we have *ideal interleaving* if $i \geq N$, where N

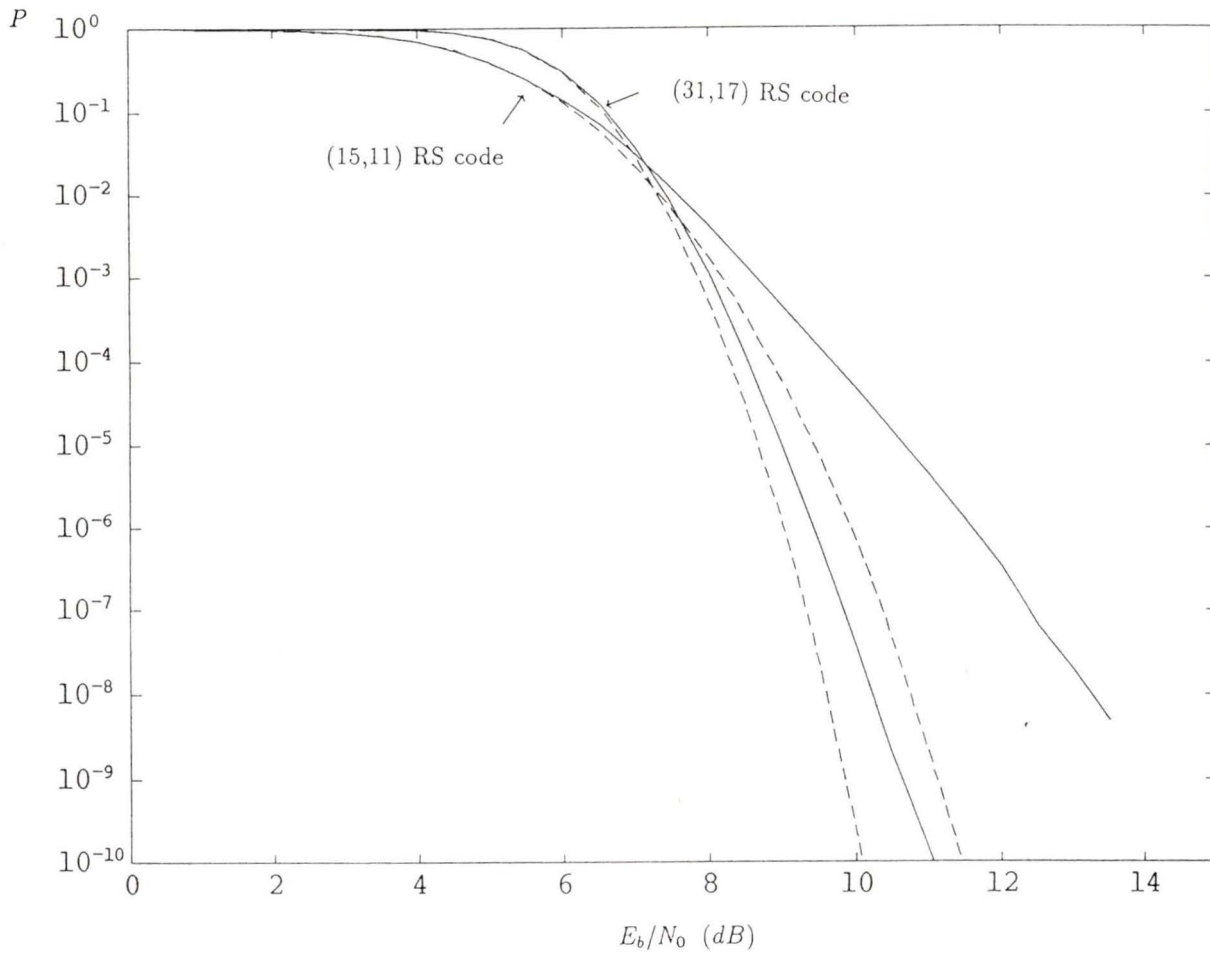


Figure 2.8: Codeword error probabilities based on the memoryless model (dashed line) and the exact expression (solid line) for BDPSK. Block length is 4 for (15, 11) RS code over $GF(2^4)$ that can correct up to two symbol errors per codeword. Block length is 5 for (31, 17) RS code over $GF(2^5)$ that can correct up to seven symbol errors per codeword. AWGN is assumed.

is the length of the codeword. Interleaving is a commonly used technique to increase the burst-error-correcting capability [8].

If we use ideal interleaving to eliminate the correlation in code symbol errors, the resultant error probability is the one based on the memoryless model. In other words, the difference between the exact error probability and the one based on the memoryless model is the gain that can be achieved with interleaving. For example, from Figure 2.8, the error probability based on the memoryless model requires 1.7 dB less in E_b/N_0 than is required by the exact one at the error probability of 10^{-6} . This implies that if we use interleaving on the code symbol basis (but not on the binary channel symbol basis), we may gain up to 1.7 dB in E_b/N_0 .

Figure 2.9 shows the results using 4-ary DPSK and (15, 11) 16-ary RS code with block length $m = 2$.

It is interesting to note that although the memoryless model is very accurate for computing the block error probability for nonbinary DPSK, it is not accurate to compute the decoded error probability. This is evident from the appreciable difference between the exact and the approximate decoded error probabilities as shown in Figure 2.9. That is, the correlation between block errors can not be ignored if the code rate is very high which makes the code ineffective against burst errors. In this case, interleaving may be required.

When the code becomes very powerful, the difference between the exact and the approximate decoded error probabilities diminishes over the range of error probabilities of interest. In this case, interleaving can be saved and so are the associated delay, the synchronization required and the implementation cost.

For nonbinary DPSK, there is a region where the approximate decoded error probability is slightly higher than the exact error probability. This makes the ap-

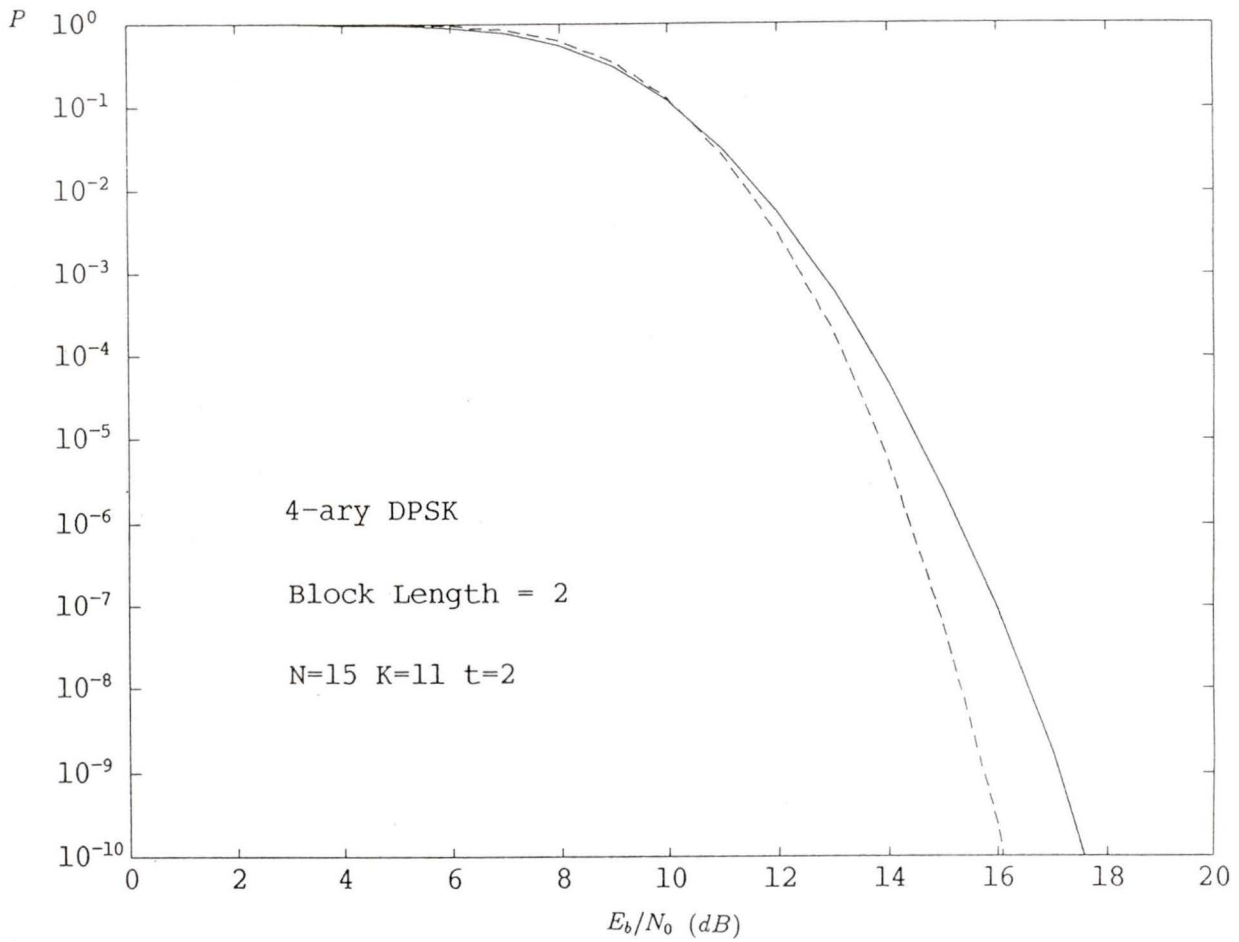


Figure 2.9: Codeword error probabilities based on the memoryless model (dashed line) and the exact expression (solid line) for 4-ary DPSK. Block length is 2. (15, 11) RS code over $GF(2^4)$ is used for correcting up to two symbol errors per codeword. AWGN is assumed.

proximate error probability under worst case PBN also slightly higher than the exact error probability which are shown in Figures 2.10 and 2.11 for 4-ary and 8-ary DPSK, respectively. The worst case decoded error probability in PBN for BDPSK is shown in Figure 2.12. From Figure 2.12 we can see that for BDPSK, the approximate and exact decoded error probabilities are almost equal. Therefore, interleaving will not provide any gain in this case.

2.4 Conclusions

We have considered the error correlation in DPSK demodulation in terms of its effects on the block and decoded error probabilities. The exact error probabilities have been derived and computed. Comparisons have been made with the approximate block and decoded error probabilities based on the memoryless model. Both the worst case PBN and AWGN have been considered.

For BDPSK in AWGN, we have found that the approximate and the exact block error probabilities are almost equal for a reasonably low error probability. But under worst case PBN, the exact block error probability is lower than the approximate block error probability. However, the approximate and exact worst case decoded error probabilities are almost equal for BDPSK.

For nonbinary DPSK, the approximate and exact block error probabilities are almost equal in both the worst case PBN and AWGN. Under worst case PBN, the approximate worst case decoded error probability is slightly higher than the exact decoded error probability.

For AWGN and for the error probability of interest, the approximate decoded error probability is lower than the exact decoded error probability. The difference

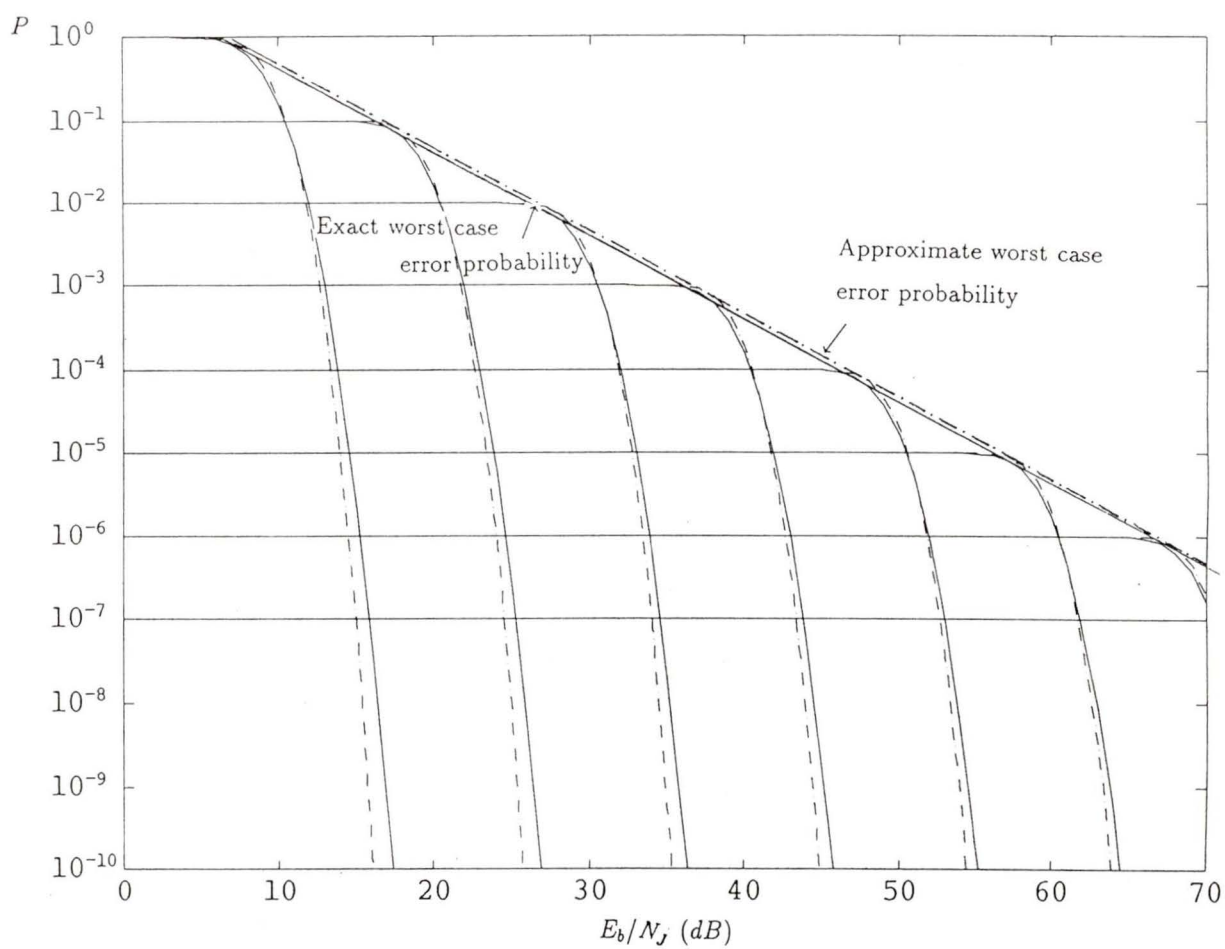


Figure 2.10: Worst case codeword error probabilities based on the memoryless model (dashdot line) and the exact expression (solid line) for 4-ary DPSK. Block length is 2. (15, 7) RS code over $GF(2^4)$ is used for correcting up to four symbol errors per codeword. AWGN is assumed.

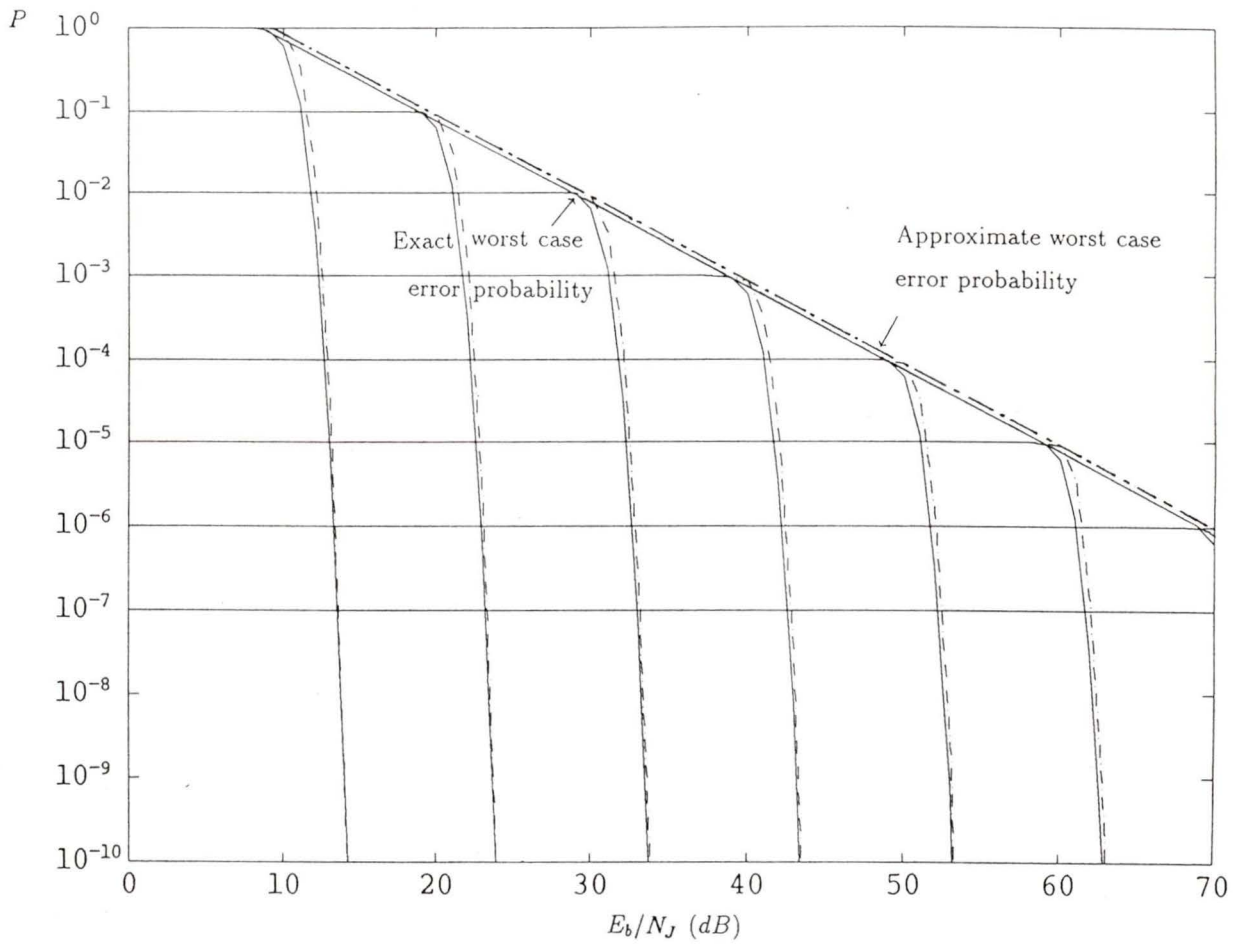


Figure 2.11: Worst case codeword error probabilities based on the memoryless model (dashdot line) and the exact expression (solid line) for 8-ary DPSK. Block length is 2. (63, 31) RS code over $GF(2^6)$ is used for correcting up to sixteen symbol errors per codeword. AWGN is assumed.

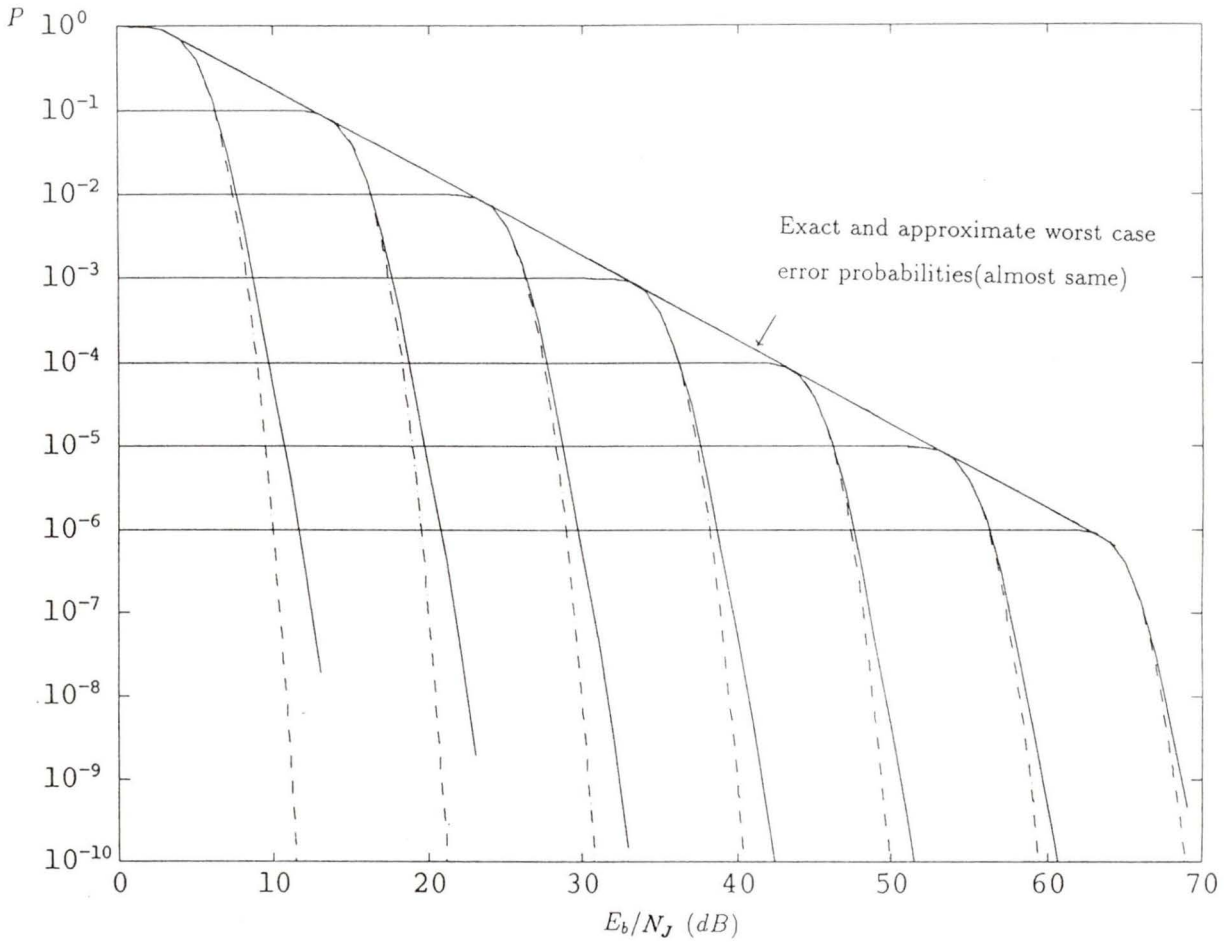


Figure 2.12: Worst case codeword error probabilities based on the memoryless model (dashdot line) and the exact expression (solid line) for BDPSK. Block length is 4. (15, 7) RS code over $GF(2^4)$ is used for correcting up to four symbol errors per codeword. AWGN is assumed. The approximate and the exact worst case error probabilities are almost equal.

is quite significant for a high rate or low redundancy code. When the code becomes very powerful, the difference diminishes.

The above results can be translated into the requirement for interleaving. Under worst case PBN, interleaving will not improve the error performance hence not needed. In AWGN, however, interleaving can provide a few dB gain in E_b/N_0 . The gain is significant for a high rate or low redundancy code. The gain decreases as the code becomes more powerful.

Chapter 3

Block and Decoded Error Probabilities of SFH/DPSK in Tone Interference and AWGN

3.1 Introduction

In last chapter, the performance of coded SFH/DPSK is analyzed with the interference being PBN and AWGN. In this chapter, we continue to study the performance of SFH/DPSK with the interference being tone jamming and AWGN.

With the presence of tone jamming, it is computationally prohibitive to compute the exact block and decoded error probability when the block length is large or the size of the code alphabet is large. In this chapter, we demonstrate the feasibility for evaluating the performance of a code of practical interest, i.e., for the RS code of alphabet size 256. In particular, we focus on the study of 8-bit blocks. The error probabilities of all 256 possible error patterns are examined, and the ‘00000000’ and ‘11111111’ block patterns are found to have the smallest and largest block error probabilities. The average block error probability is also calculated. We then proceed to evaluate the performance of an RS code over $GF(2^8)$, which is one of

the promising candidates for SFH/DPSK. The overall decoded error probability is computed with the error correlation in DPSK demodulation taken into account. The ‘range’ of decoded error probabilities is determined by assuming that every code symbol comes from the ‘00000000’ block pattern or the ‘11111111’ block pattern. To investigate the effect of error correlation due to DPSK demodulation and tone jamming, the range of decoded error probabilities obtained with ideal interleaving is evaluated and compared with the case where interleaving is not applied. To study the effect of different coding schemes on system performance, we compare the decoded error probabilities of codes with different code rates, and a nearly optimum code rate for the RS code of length 255 is found for SFH/DPSK systems with ideal interleaving. To investigate the anti-jamming capability of SFH/DPSK, decoded performance under worst case tone jamming is also presented.

In this chapter, it is assumed that the frequency hopping rate is slow enough that each codeword can be completely transmitted over one hop. Although the error probabilities corresponding to 8-bit blocks and RS codes of length 255 are presented here for example, the analytical approach developed here is also applicable to other coding schemes.

3.2 Block Error Probability in Tone Interference and AWGN

As illustrated earlier, due to the correlation inherent to DPSK demodulation, a phase error affecting a signal vector subjects the two consecutive decisions related to this vector to errors. Decision errors can not be viewed as being independent. Therefore the block error probability p_E is given by

$$p_E = 1 - p_{c1}p_{c2|c1}p_{c3|c2} \cdots p_{ci|c(i-1)} \cdots p_{cm|c(m-1)}, \quad (3.1)$$

where p_{c1} denotes the probability that the first symbol in the block is correct, $p_{ci|c(i-1)}$ denotes the probability that the i th symbol is correct conditioned on the previous symbol being correct, and m is the length of the block.

Unlike AWGN, where every decision has the same error probability, tone jamming does not affect every possible transmitted differential phase equally. In general, different blocks have different error probabilities. We must evaluate the probability p_{ci} and the conditional probabilities $p_{ci|c(i-1)}$ for all possible differential phases. The approach to be employed to deal with simultaneous tone interference and AWGN is to add white Gaussian noise to the signal vectors which have already been perturbed by a jamming tone with a fixed initial phase. We then average this result over the pdf of the jamming tone initial phase to obtain the error performance in the presence of the two interferences.

The transmitted DPSK signal vector can be represented in complex form as

$$S^{(i)} = Ae^{j(\theta + \theta_T^{(i-1)})}, \quad (3.2)$$

where $\theta_T^{(i-1)}$ is the accumulated phase in the $(i-1)$ th signaling interval and θ is the differential phase transmitted in the i th signaling interval. The jamming tone is represented as

$$J = Ie^{j\theta_J}, \quad (3.3)$$

where θ_J is a random phase uniformly distributed in an interval of length 2π .

Thus the jamming-tone-corrupted signal vector is represented as

$$\begin{aligned} S_J^{(i)} &= Ae^{j(\theta+\theta_T^{(i-1)})} + Ie^{j\theta_J}, \\ &= A_J e^{j(\theta+\theta_T^{(i-1)}+\delta_J^{(i)})}, \end{aligned} \quad (3.4)$$

where $\delta_J^{(i)}$ indicates the phase deviation caused by the jamming tone in the i th signaling interval.

Suppose that signal vectors $S^{(i-1)}$ and $S^{(i)}$ are transmitted successively. After being jammed, the resultant signal vectors $S_J^{(i-1)}$ and $S_J^{(i)}$ will have a phase separation given by

$$\Delta\Phi_J = \arg(S_J^{(i)} S_J^{(i-1)*}) = \theta + \delta_J^{(i)} - \delta_J^{(i-1)}, \quad (3.5)$$

where the function arg returns the principal value in the range $(-\pi, \pi]$.

The two signal vectors are then perturbed by independent Gaussian noise, causing a phase separation ϕ at the receiver. Suppose that the DPSK demodulator makes the right decision if ϕ lies in the decision region $\phi_1 \leq \phi \leq \phi_2$. Then the probability of correct reception conditioned on the signal vectors being jammed is [7]

$$p_{ci|\theta_J} = p_r(\phi_1 \leq \phi \leq \phi_2 | \theta_J) = \begin{cases} F(\phi_2) - F(\phi_1) + 1 & \phi_1 \leq \Delta\Phi_J \leq \phi_2 \\ F(\phi_2) - F(\phi_1) & \phi_1 > \Delta\Phi_J \text{ or } \phi_2 < \Delta\Phi_J \end{cases} \quad (3.6)$$

where

$$F(\phi) = \frac{W \sin(\Delta\Phi_J - \phi)}{4\pi} \int_{-\pi/2}^{\pi/2} \frac{e^{-G}}{G} dt,$$

and

$$G = U - V \sin t - W \cos(\Delta\Phi_J - \phi) \cos t.$$

The constants U, V and W are

$$\begin{aligned} U &= 0.5(\sigma^{(i)} + \sigma^{(i-1)}), \\ V &= 0.5(\sigma^{(i)} - \sigma^{(i-1)}), \\ W &= \sqrt{U^2 - V^2}, \end{aligned}$$

where

$$\sigma^{(i)^2} = \frac{|A_J^{(i)}|^2}{2N_0}.$$

Here $A_J^{(i)}$ is the amplitude of the jammed signal vector in the i th signaling interval. N_0 is the one-sided power spectral density of the white Gaussian noise.

We now derive the joint probability for two block symbols to be correct conditioned on their being jammed by the tone described in Eq. (3.3). In the last chapter, for a signal vector disturbed by AWGN, the pdf of the phase deviation from the original phase is given by Eq. (2.2). By applying Eq. (2.2) to the tone jammed signal vector in Eq. (3.4), the pdf of the phase error caused by a tone with a given θ_J and AWGN is

$$\begin{aligned} h(\delta^{(i)}|\theta_J) &= f(\delta^{(i)} - \delta_J^{(i)}) \\ &= \frac{1}{2\pi} e^{-R^{(i)}} + \frac{1}{2} \sqrt{\frac{R^{(i)}}{\pi}} e^{-R^{(i)} \sin^2(\delta^{(i)} - \delta_J^{(i)})} \cos(\delta^{(i)} - \delta_J^{(i)}) \end{aligned}$$

$$\times [1 + \text{erf}(\sqrt{R^{(i)}} \cos(\delta^{(i)} - \delta_J^{(i)}))],$$

$$\delta^{(i)}, \delta_J \in [-\pi, \pi], \quad (3.7)$$

where $R^{(i)} = E_{sJ}^{(i)}/N_0$. Here $E_{sJ}^{(i)}$ is the energy of the i th signal vector after being jammed.

Assuming that three signal vectors $S^{(i-1)}$, $S^{(i)}$ and $S^{(i+1)}$ are transmitted over three successive signaling intervals, two decisions are made in the demodulator based on the phase difference between the received signal vectors $Y^{(i-1)}$, $Y^{(i)}$, and $Y^{(i+1)}$.

Let $\delta^{(i-1)}$, $\delta^{(i)}$ denote the phase difference between the received and transmitted signal vectors over the $(i-1)$ th and i th signaling intervals,

$$\delta^{(i-1)} = \arg(Y^{(i-1)}S^{(i-1)*}), \quad (3.8)$$

$$\delta^{(i)} = \arg(Y^{(i)}S^{(i)*}). \quad (3.9)$$

The phase difference between two successive received signal vectors can be expressed as follows:

$$\begin{aligned} \phi^{(i-1)} &= \arg(Y^{(i)}Y^{(i-1)*}), \\ &= \theta^{(i)} + \delta^{(i)} - \delta^{(i-1)}. \end{aligned} \quad (3.10)$$

$$\begin{aligned} \phi^{(i)} &= \arg(Y^{(i+1)}Y^{(i)*}), \\ &= \theta^{(i+1)} + \delta^{(i+1)} - \delta^{(i)}. \end{aligned} \quad (3.11)$$

Denote the decision region for the $(i-1)$ th decision by $(\phi_1^{(i-1)}, \phi_2^{(i-1)})$, and that for the i th decision by $(\phi_1^{(i)}, \phi_2^{(i)})$. Then given a phase error $\delta^{(i)}$ in the i th signal vector, the region for $\delta^{(i-1)}$ in which the $(i-1)$ th decision can be correctly made is

$(a^{(i-1)}, b^{(i-1)}) = (\delta^{(i)} + \theta^{(i)} - \phi_2^{(i-1)}, \delta^{(i)} + \theta^{(i)} - \phi_1^{(i-1)})$. The corresponding region for $\delta^{(i+1)}$ is $(a^{(i+1)}, b^{(i+1)}) = (\phi_1^{(i)} - \theta^{(i+1)} + \delta^{(i)}, \phi_2^{(i)} - \theta^{(i+1)} + \delta^{(i)})$.

The probability for the $(i-1)$ th decision to be correct conditioned on the phase error $\delta^{(i)}$ in the i th signal vector is then

$$\begin{aligned} p_{c(i-1)|\theta_J, \delta^{(i)}} &= \int_{a^{(i-1)}}^{b^{(i-1)}} h(\delta^{(i-1)}|\theta_J) d\delta^{(i-1)} \\ &= \frac{1}{2\pi} e^{-R^{(i-1)}} + \frac{1}{2} \sqrt{\frac{R^{(i-1)}}{\pi}} e^{-R^{(i-1)} \sin^2(\delta^{(i-1)} - \delta_J^{(i-1)})} \cos(\delta^{(i-1)} - \delta_J^{(i-1)}) \\ &\quad \times [1 + \operatorname{erf}(\sqrt{R^{(i-1)}} \cos(\delta^{(i-1)} - \delta_J^{(i-1)}))] d\delta^{(i-1)}. \end{aligned} \quad (3.12)$$

Similarly, the conditional probability for the i th decision to be correct is

$$\begin{aligned} p_{ci|\theta_J, \delta^{(i)}} &= \int_{a^{(i+1)}}^{b^{(i+1)}} h(\delta^{(i+1)}|\theta_J) d\delta^{(i+1)} \\ &= \frac{1}{2\pi} e^{-R^{(i+1)}} + \frac{1}{2} \sqrt{\frac{R^{(i+1)}}{\pi}} e^{-R^{(i+1)} \sin^2(\delta^{(i+1)} - \delta_J^{(i+1)})} \cos(\delta^{(i+1)} - \delta_J^{(i+1)}) \\ &\quad \times [1 + \operatorname{erf}(\sqrt{R^{(i+1)}} \cos(\delta^{(i+1)} - \delta_J^{(i+1)}))] d\delta^{(i+1)}. \end{aligned} \quad (3.13)$$

Due to the independent nature of AWGN, the probabilities of the $(i-1)$ th decision being correct and the i th decision being correct are independent conditioned on the phase error in the i th signal vector. Therefore, the probability for two consecutive decisions to be correct conditioned on a phase error $\delta^{(i)}$ in the i th signal vector, and their being jammed by a tone with a fixed initial phase θ_J is

$$p_{c(i-1)ci|\delta^{(i)}, \theta_J} = p_{c(i-1)}(\delta^{(i)}, \theta_J) \times p_{ci}(\delta^{(i)}, \theta_J). \quad (3.14)$$

By averaging the above expression over the pdf of $\delta^{(i)}$, the probability for the

occurrence of two adjacent correct decisions conditioned on their being jammed by a tone with a fixed initial phase is given by

$$p_{c(i-1)ci|\theta_J} = \int_{-\pi}^{\pi} p_{c(i-1)ci}(\delta^{(i)}, \theta_J) h(\delta^{(i)}|\theta_J) d\delta^{(i)}. \quad (3.15)$$

We now average Eq. (3.6) and Eq. (3.15), respectively, over the pdf of the jamming tone initial phase, which is assumed to be uniformly distributed over $(-\pi, \pi]$. The probability p_{ci} for one decision to be correct, and the probability $p_{c(i-1)ci}$ for two decisions to be correct are

$$p_{ci} = \int_{-\pi}^{\pi} p_{ci|\theta_J} \times \frac{1}{2\pi} d\theta_J, \quad (3.16)$$

$$p_{c(i-1)ci} = \int_{-\pi}^{\pi} p_{c(i-1)ci|\theta_J} \times \frac{1}{2\pi} d\theta_J. \quad (3.17)$$

The probability for the i th decision to be correct provided the previous one is correct is therefore

$$p_{ci|c(i-1)} = \frac{p_{c(i-1)ci}}{p_{c(i-1)}}. \quad (3.18)$$

The block error probability can finally be obtained by substituting Eq. (3.16) and Eq. (3.18) into Eq. (3.1). The average block error probability can be found by adding the probabilities for all possible block error patterns and dividing the sum by the number of error patterns.

A Fortran program was written to carry out the above calculations for binary DPSK with block length 8. Symbol '0' is assumed to be represented by the differential phase 0, and symbol '1' is represented by the differential phase ' π '. The

computation load can be greatly reduced since that there are only four adjacent block symbol patterns to be considered, i.e., 00, 01, 10, and 11. Since Eq. (2.2) is used repeatedly in different forms, the computation speed is greatly enhanced by storing some of the intermediate values. Special caution must be taken when carrying out the integration in Eq. (3.6), for the integrand has a singularity at $\arctan\left(\frac{v}{w \cos(\Delta\Phi - \phi)}\right)$.

The result of the 8-bit block error probability for binary DPSK is shown in Figure 3.1. E_s/N_J is the broad band signal-to-jamming ratio (*SJR*), where N_J is the jamming power spectral density and E_s is the energy of each DPSK symbol. It is seen that the block pattern ‘00000000’ has the lowest error probability. This is due to the fact that symbol ‘0’ is represented by two parallel signal vectors which remain parallel after being jammed by a tone. In other words, symbol ‘0’ is immune to tone jamming. The block pattern that is most susceptible to error is ‘11111111’. A jamming tone can significantly alter the differential phase π representing symbol ‘1’. The average block error probability is also calculated. These results serve as the basis for the evaluation of decoded error probabilities in the next section.

3.3 Decoded Error Probability

In this section, we study the probability for bounded distance decoding failure in tone jamming and AWGN.

In AWGN, each block has equal error probability, therefore different codewords have equal error probabilities given their error distributions are the same. But in tone interference and AWGN, different codewords may have different error probabilities even if they have identical code symbol error patterns. This is because the effect

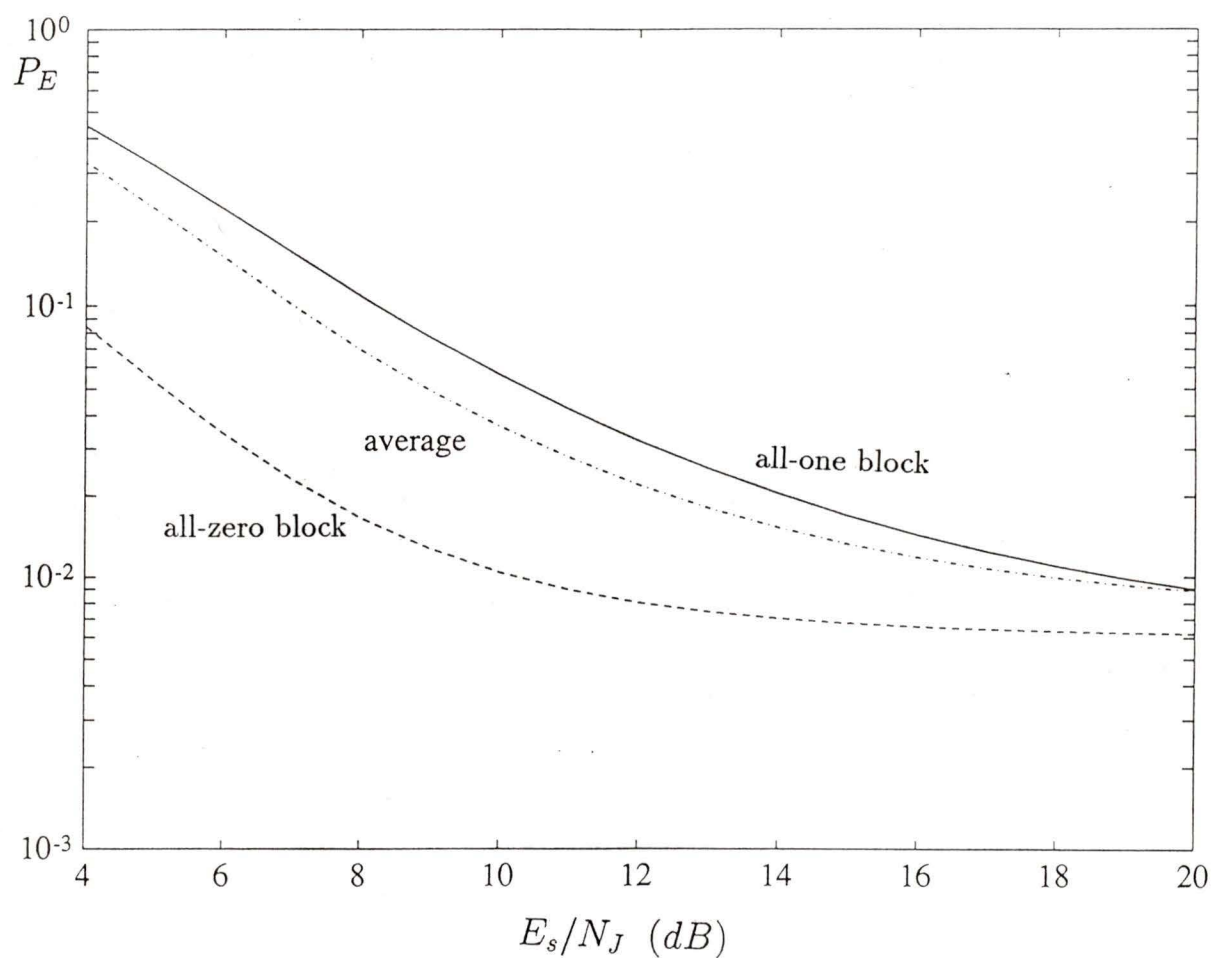


Figure 3.1: Block error probabilities for BDPSK in both tone interference and AWGN. The block error probabilities for the all-zero block pattern (dashed line), the all-one block pattern (solid line), and the average block error probability (dash-dotted line) are shown. $m = 8$, $SNR = 8dB$.

of tone jamming depends heavily on the specific differential phases transmitted.

To calculate the exact decoding failure probability, the number of error patterns that should be taken into account will be prohibitively large when N and K are large. It is computationally difficult, if not impossible, to examine all the codewords one by one to obtain the corresponding error probabilities. As a partial solution, we try to evaluate the error probabilities of some typical codewords with the hope that the results can provide an insight into the decoded error performance of other codewords.

In the last section, the ‘00000000’ and ‘11111111’ block patterns are found to have the smallest and largest block error probabilities. As a natural choice, we consider the decoded error performance of the codeword consisting exclusively of ‘00000000’ patterns, and that of the codeword consisting of only ‘11111111’ patterns. We name the decoded error probabilities of these two codewords as a *range* of the decoded error performance. However, we must realize that they are not bounds of the decoded error performance. The range is used just as an indication of the decoded error probabilities for other codewords.

Since the all-zero and all-one codewords are made up of exactly same blocks: ‘00000000’ and ‘11111111’, respectively, it is unnecessary to distinguish between the error probabilities of different blocks.

Formulations for evaluating the decoded error probability were given in Section 2.3. The same approach is taken here with the additional condition that the codeword is already interrupted by a jamming tone with a fixed initial phase. By replacing the probabilities in the equations of Section 2.3 by corresponding conditional probabilities, e.g., p_E by $p_E(\theta_J)$, the decoded error probability conditioned on the codeword being jammed by jamming tone $J = Ie^{j\theta_J}$ is

$$P(\theta_J) = \sum_{i=t+1}^N p(N, i|\theta_J), \quad (3.19)$$

where N and t are as defined before.

The codeword probability can be obtained by averaging the above equation over the pdf of jamming tone initial phase, i.e.

$$P = \int_{-\pi}^{\pi} P(\theta_J) \frac{1}{2\pi} d\theta_J. \quad (3.20)$$

Figures 3.2 and 3.3 show the ranges of decoded error probabilities for (255, 195) and (255, 223) RS codes, respectively, with a signal-to-noise ratio of 10dB. Figure 3.2 indicates that the decoded error probability for the codeword consisting of the block pattern ‘00000000’ is always better than that for ‘11111111’. We may assume that the decoded error probabilities for other codewords fall between these two extremes. In Figure 3.3, a crossing point is observed between the two curves. The reason is that although block pattern ‘00000000’ has the least probability of error, the correlation between blocks is much stronger than that between the patterns of ‘11111111’ when the signal-to-jamming ratio is larger than a certain value. With the more powerful (255, 195) code, the pattern ‘00000000’ is always better than the pattern ‘11111111’. The (255, 223) code exhibits a stronger correlation among all-0 patterns, causing more bursty errors exceeding the error correction capability of the code. By comparing Figure 3.2 with Figure 3.3, it can be seen that the use of a more powerful code may reduce the range of decoded error probabilities, but the reduction depends on the signal-to-jamming ratio used.

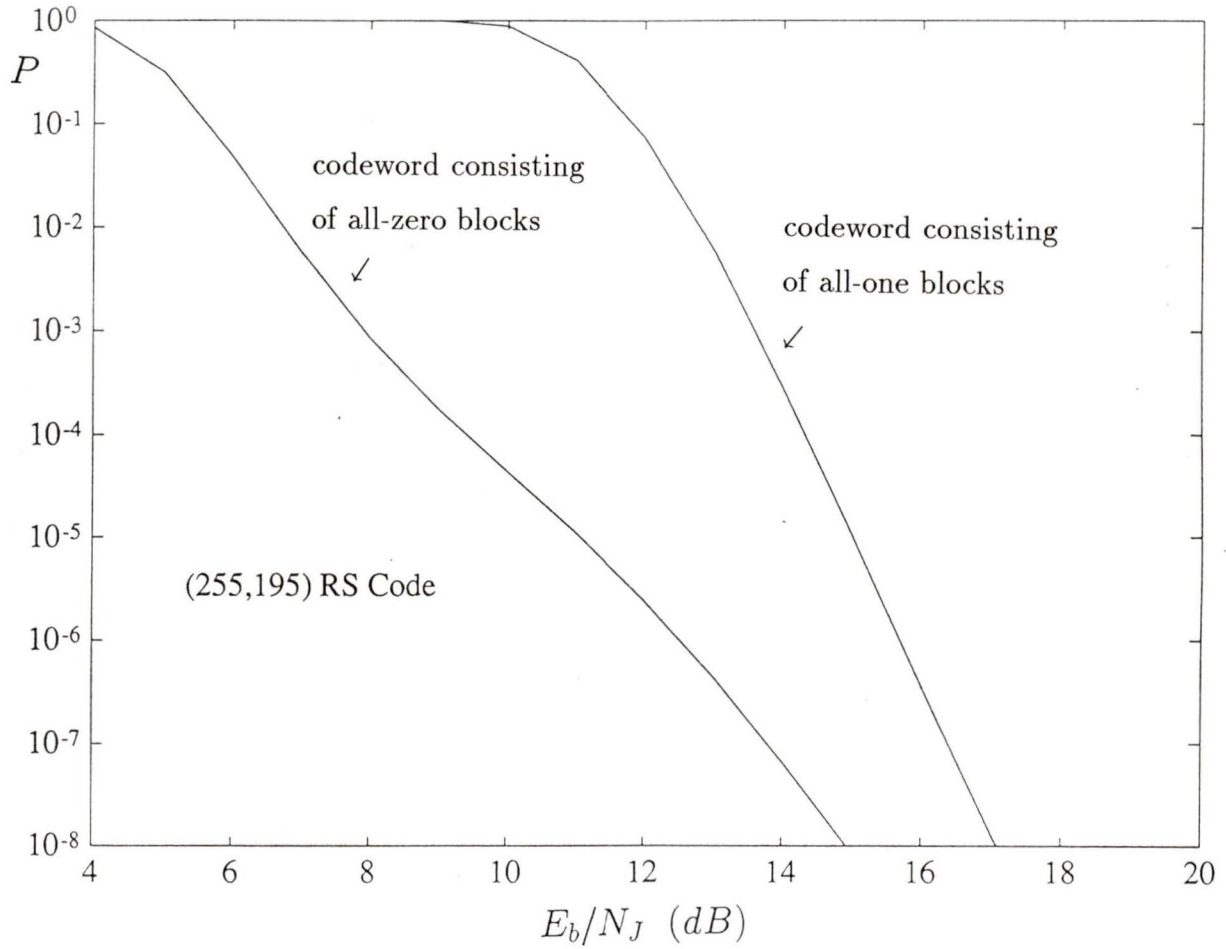


Figure 3.2: The range of the decoded error probabilities for (255, 195) RS code over $GF(2^8)$ that can correct up to 30 errors. $SNR = 10dB$.

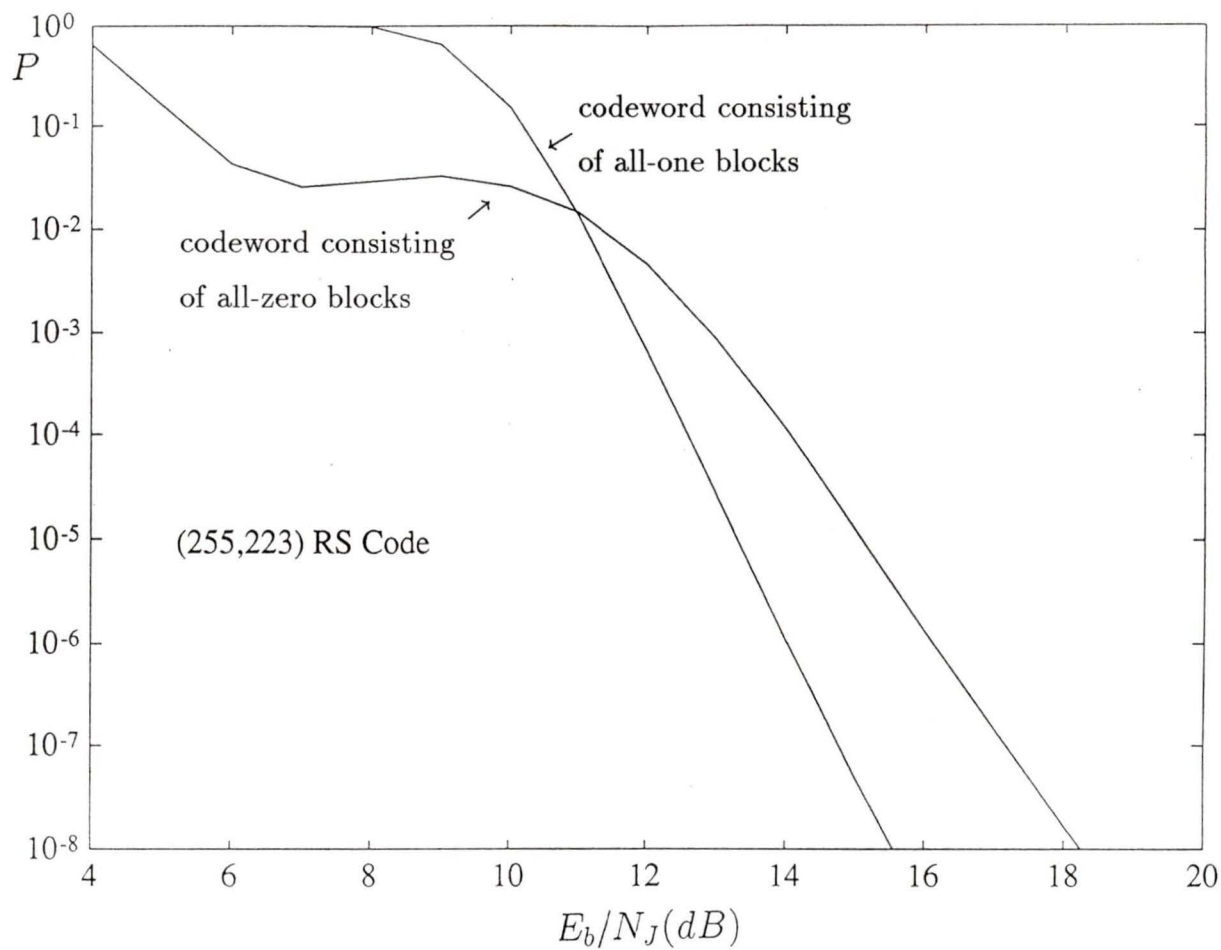


Figure 3.3: The range of the decoded error probabilities for (255, 223) RS code over $GF(2^8)$ that can correct up to 16 errors. $SNR = 10dB$.

3.4 Effect of Interleaving and Performance under Worst Case Tone Jamming

As the employment of an interleaving technique can provide some performance gain in certain cases where the interference is PBN and AWGN, it is natural that we are also interested in the effect of interleaving when the interference is tone jamming and AWGN. With ideal interleaving, code symbol errors are considered to occur independently. Then the decoding failure probability is given by the memoryless model as used in the last chapter,

$$P = \sum_{i=t+1}^N \binom{N}{i} p_E^i (1 - p_E)^{N-i}, \quad (3.21)$$

where p_E denotes the block error probability.

The decoded error probabilities for the codewords formed by the ‘00000000’ and ‘11111111’ block patterns and the average decoded error probability are shown in Figure 3.4, 3.5, 3.6, and 3.7. Figures 3.4 and 3.5 indicate that while interleaving does not greatly reduce the decoded error probability for the all-one codeword, it drastically reduces the error probability for the all-zero codeword. By comparing Figures 3.6 and 3.7, we see that with the application of interleaving, the use of a lower rate code does not necessarily give better performance. In Figure 3.8, the average decoded error probabilities for codes with different rates are compared with the interleaving technique adopted. It can be seen that the code rate has a significant effect on system performance. In fact, there exists an optimum code rate for specific values of SNR and SJR . Figure 3.8 demonstrates a case in which the (255, 223) RS code provides better performance than RS codes of any other rates on $GF(2^8)$.

To understand the anti-jamming ability of SFH/DPSK in tone jamming and

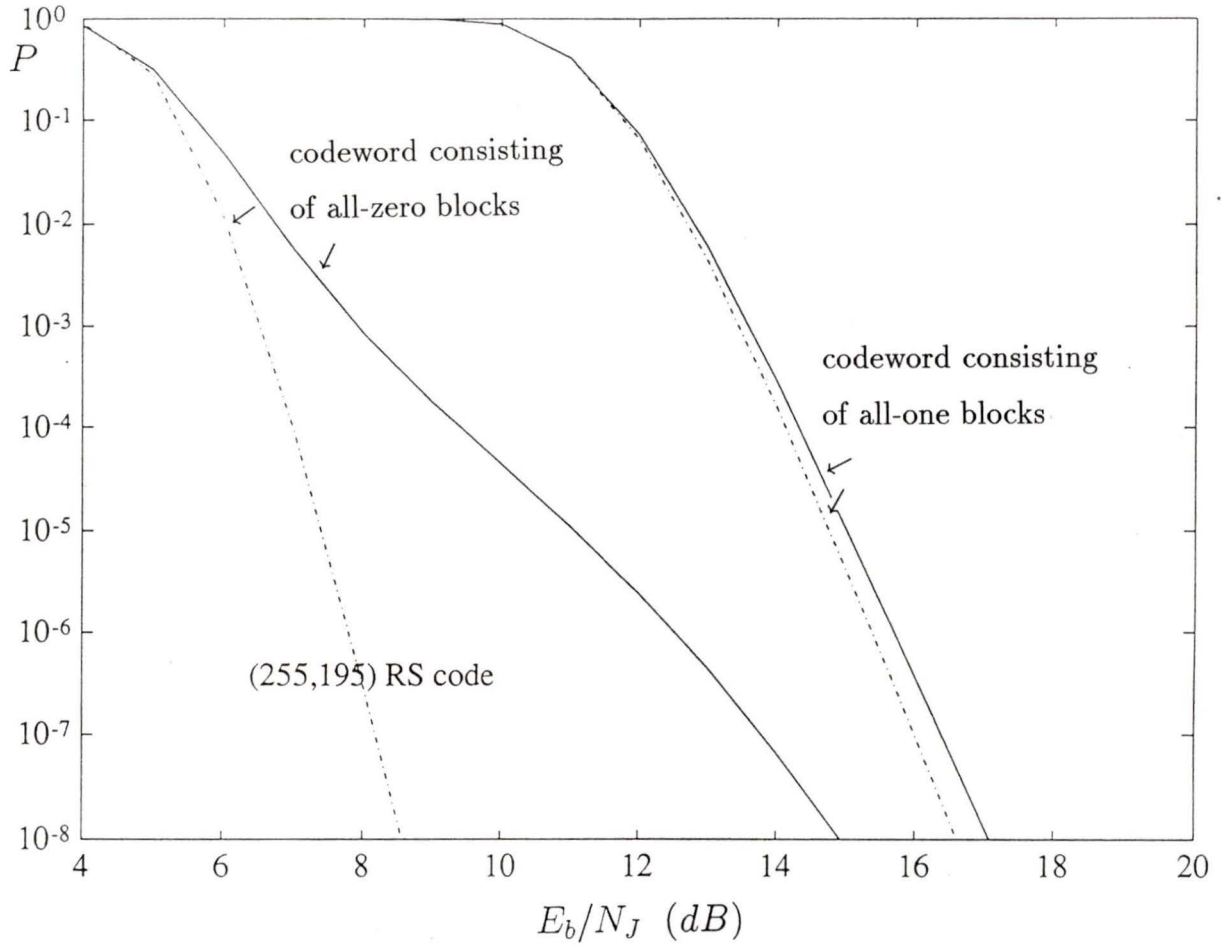


Figure 3.4: The range of the decoded error probabilities with ideal interleaving (dash-dotted line) and without interleaving (solid line). The RS code (255,195) over $GF(2^8)$ is used to correct up to 30 errors. $SNR = 10dB$.

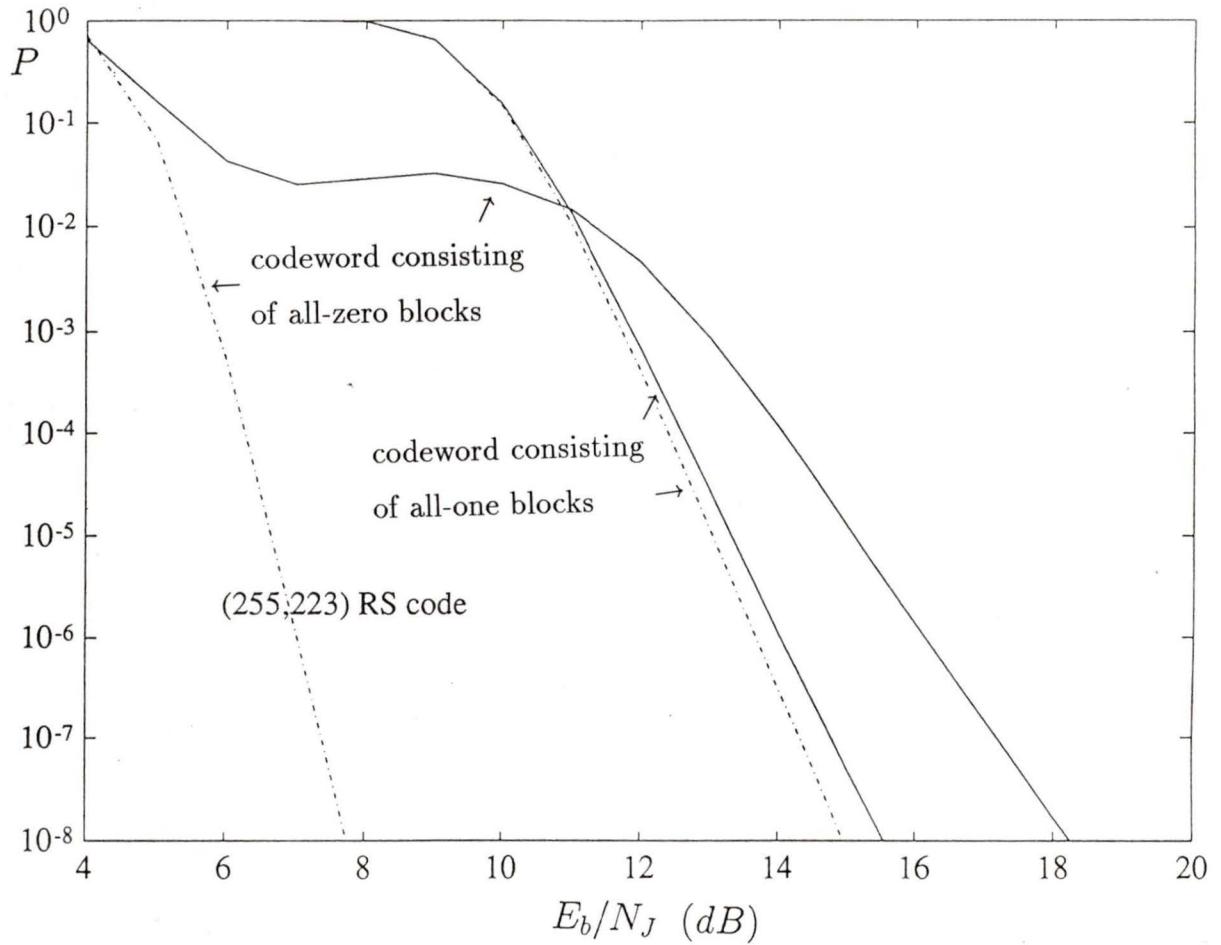


Figure 3.5: The range of the decoded error probabilities with interleaving (dash-dotted line) and without interleaving (solid line). The RS code (255, 223) over $GF(2^8)$ is used to correct up to 16 errors. $SNR = 10dB$.

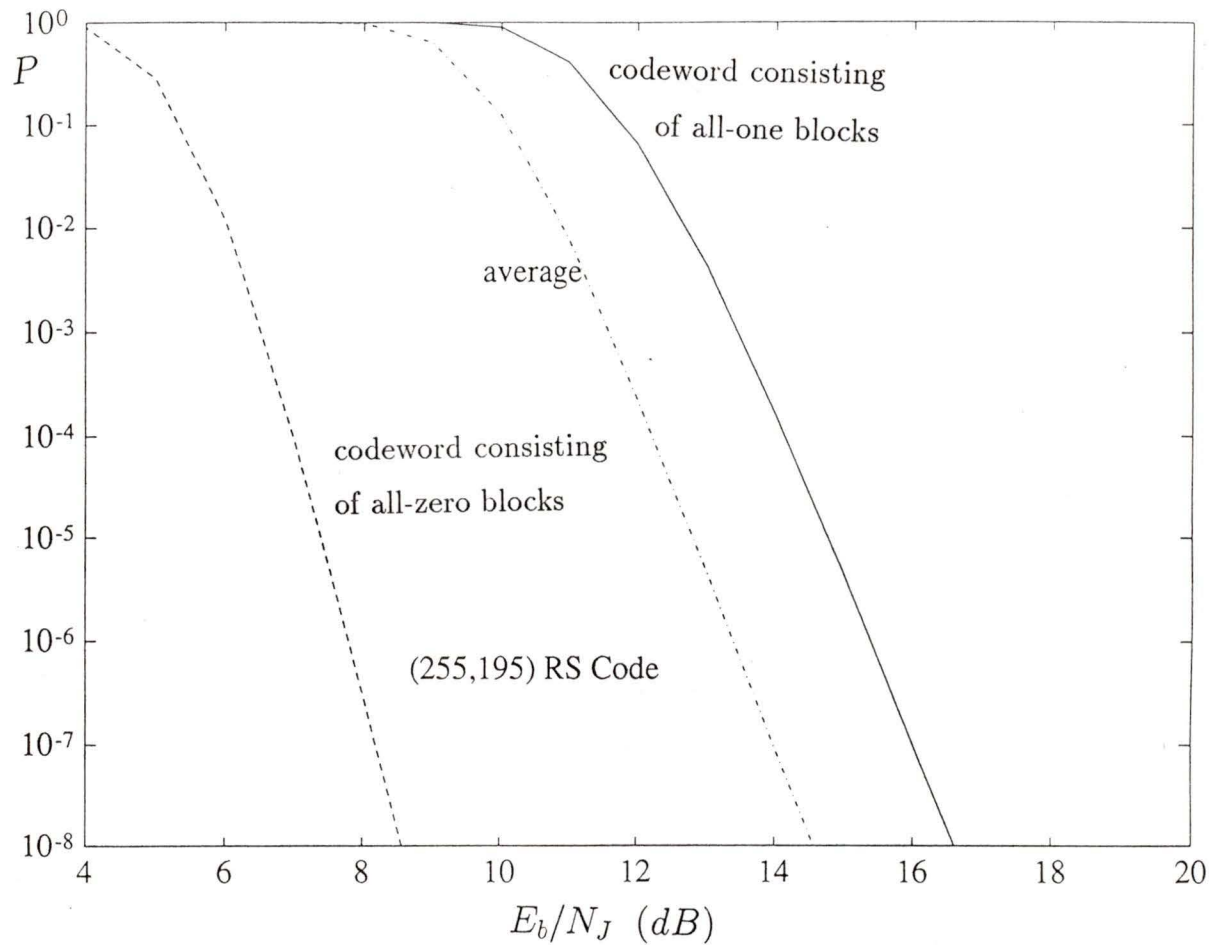


Figure 3.6: The decoded error probabilities with interleaving. The RS code (255,195) is used which can correct up to 30 errors. The all-zero codeword error probability (dashed line), the average decoded error probability (dash-dotted line), and the all-one codeword error probability (solid line) are shown. $SNR = 10dB$.

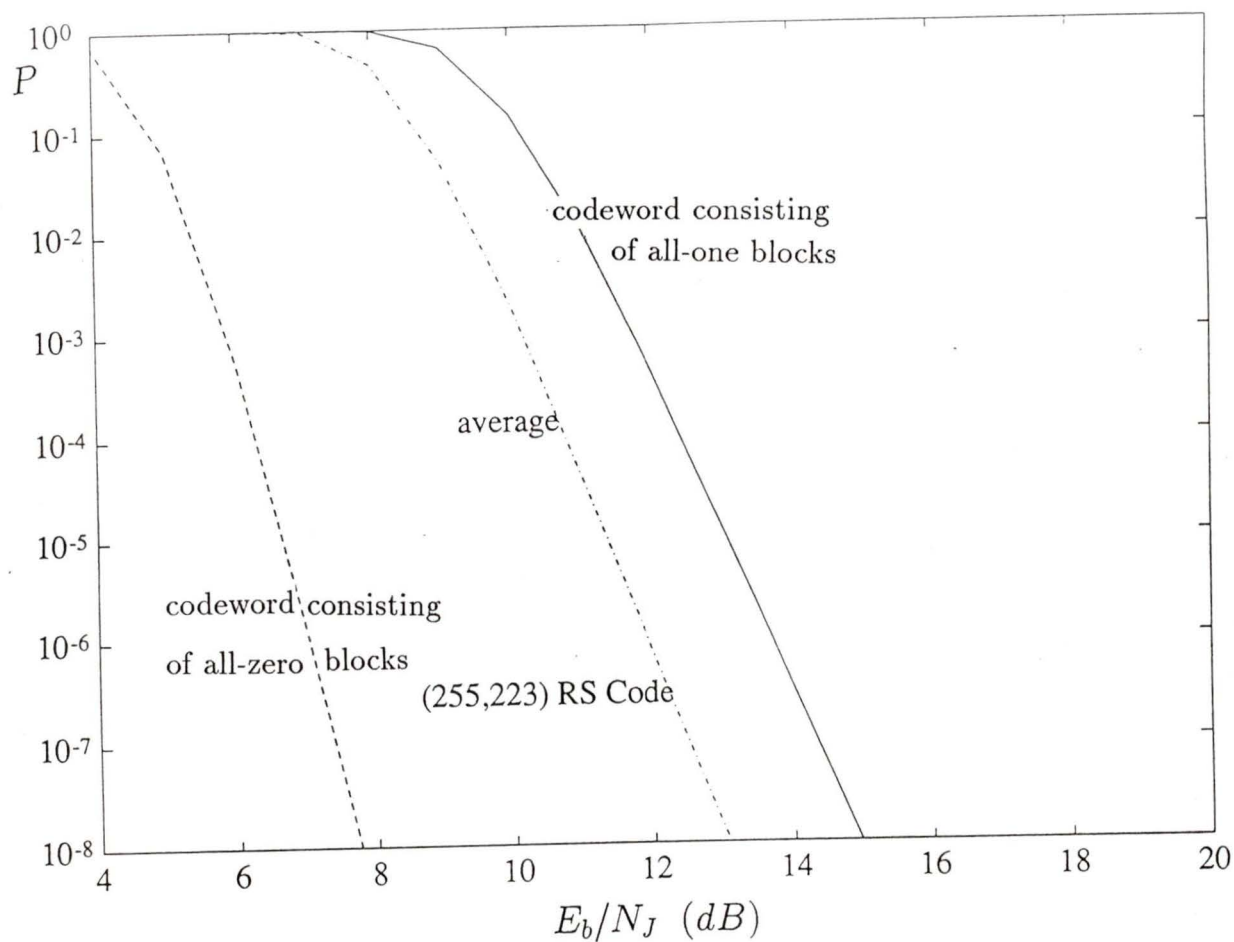


Figure 3.7: The decoded error probabilities with interleaving. The RS code (255, 223) is used which can correct up to 16 errors. The all-zero codeword error probability (dashed line), the average decoded error probability (dash-dotted line), and the all-one codeword error probability (solid line) are shown. $SNR = 10dB$.

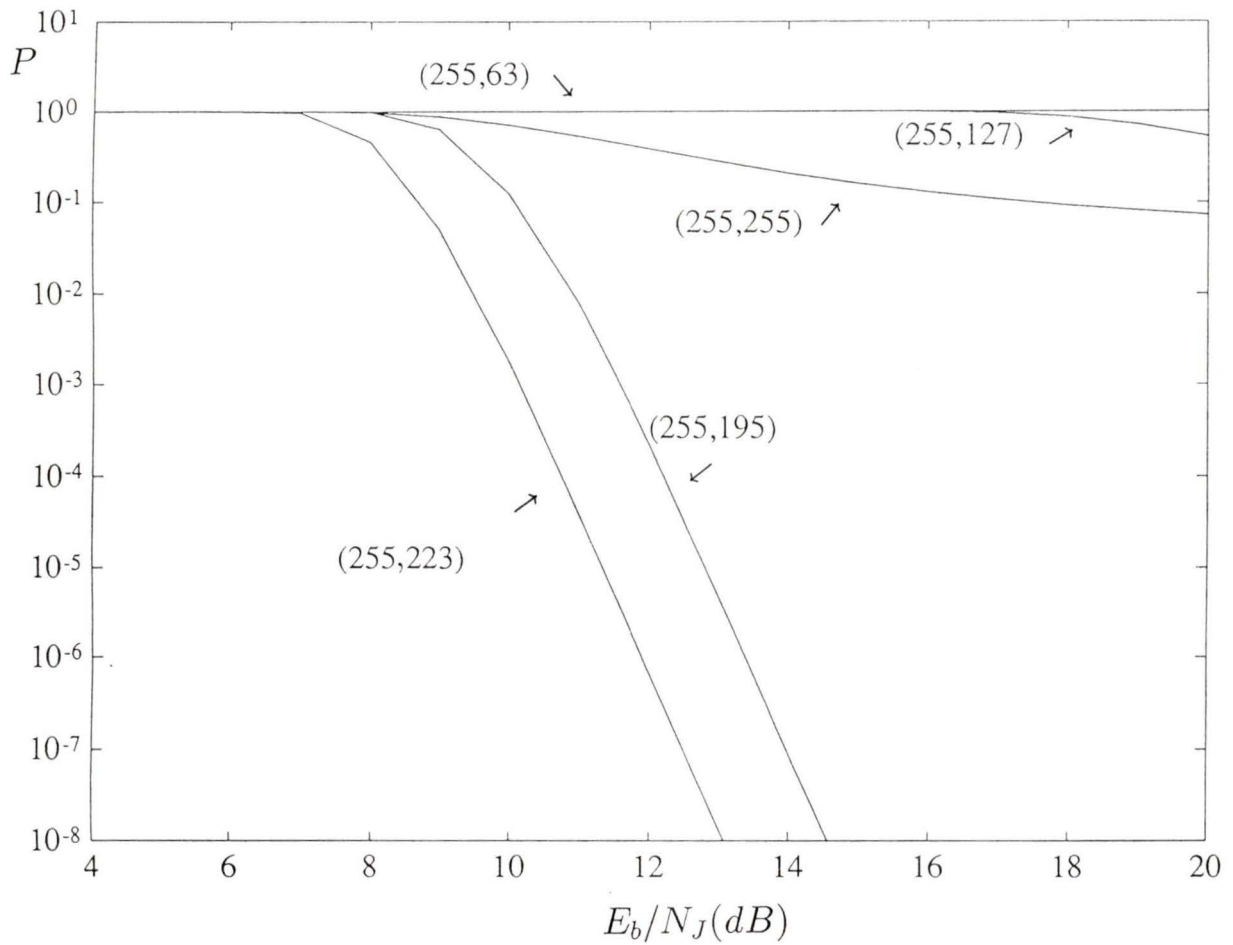


Figure 3.8: The comparison of average decoded error probabilities with interleaving. The RS codes over $GF(2^8)$ with different code rates are chosen. $SNR = 10dB$.

AWGN, we now consider the decoded error performance under worst case tone jamming.

As discussed in [10], the probability ρ for one signal vector being jammed is

$$\rho = \frac{1}{\log_2 M \beta^2 E_s / N_J}, \quad (3.22)$$

where $\beta (= \frac{I}{A})$ denotes the ratio of the amplitude of the jamming tone to that of the signal vector. E_s / N_J is the equivalent broad band signal-to-jamming ratio. M is the number of possible differential phases.

Suppose that the decoded error probability in AWGN alone is $P(E_s / N_0)$, and that in combined tone jamming and AWGN is $P(E_s / N_0, E_s / N_J)$. Then the overall decoded error probability over the whole frequency band is

$$P = (1 - \rho) \times P(E_s / N_0) + \rho \times P(E_s / N_0, \rho E_s / N_J). \quad (3.23)$$

Finding the worst case ρ is as done in the last chapter, i.e. plotting a group of curves of decoded error probabilities versus signal-to-jamming ratio, and taking the upper envelope of these curves.

The average decoded error probabilities under worst case tone jamming for the (255, 195) and (255, 223) RS codes are shown in Figures 3.9 and 3.10. By comparing these two figures, we see that although the (255, 223) RS code provides better performance than the (255, 195) RS code when ρ is fixed, it does not appreciably improve the performance under worst case tone jamming. The reason is that the worst case jamming always yields a performance corresponding to the region where the decoded error probability is still very high, i.e., where most error patterns are not correctable and therefore codes of different rates provide similar performance.

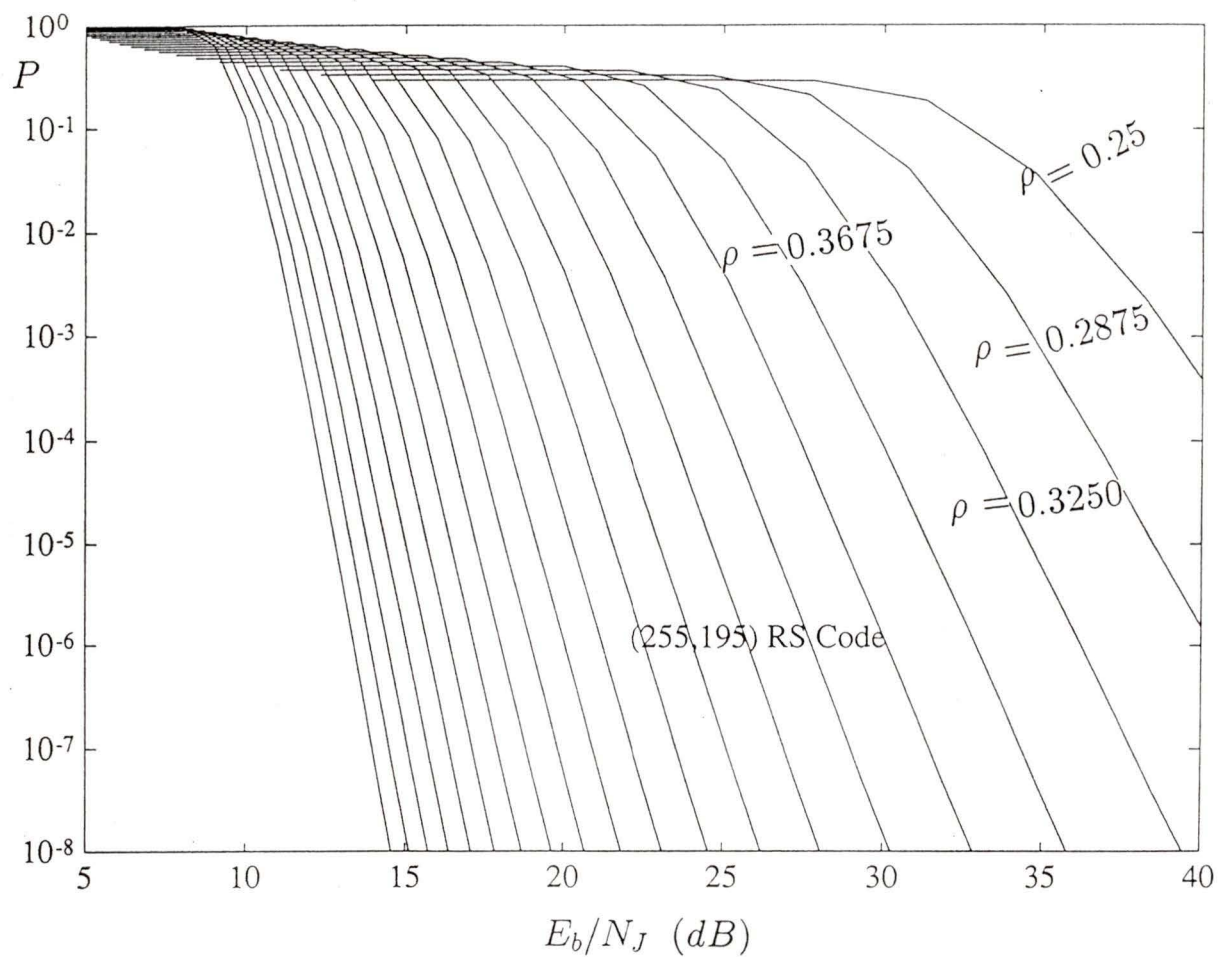


Figure 3.9: The average decoded error probabilities under worst case tone jamming. Ideal interleaving is applied. (255, 195) RS code over $GF(2^8)$ is used to correct up to 30 errors. $SNR = 10dB$.

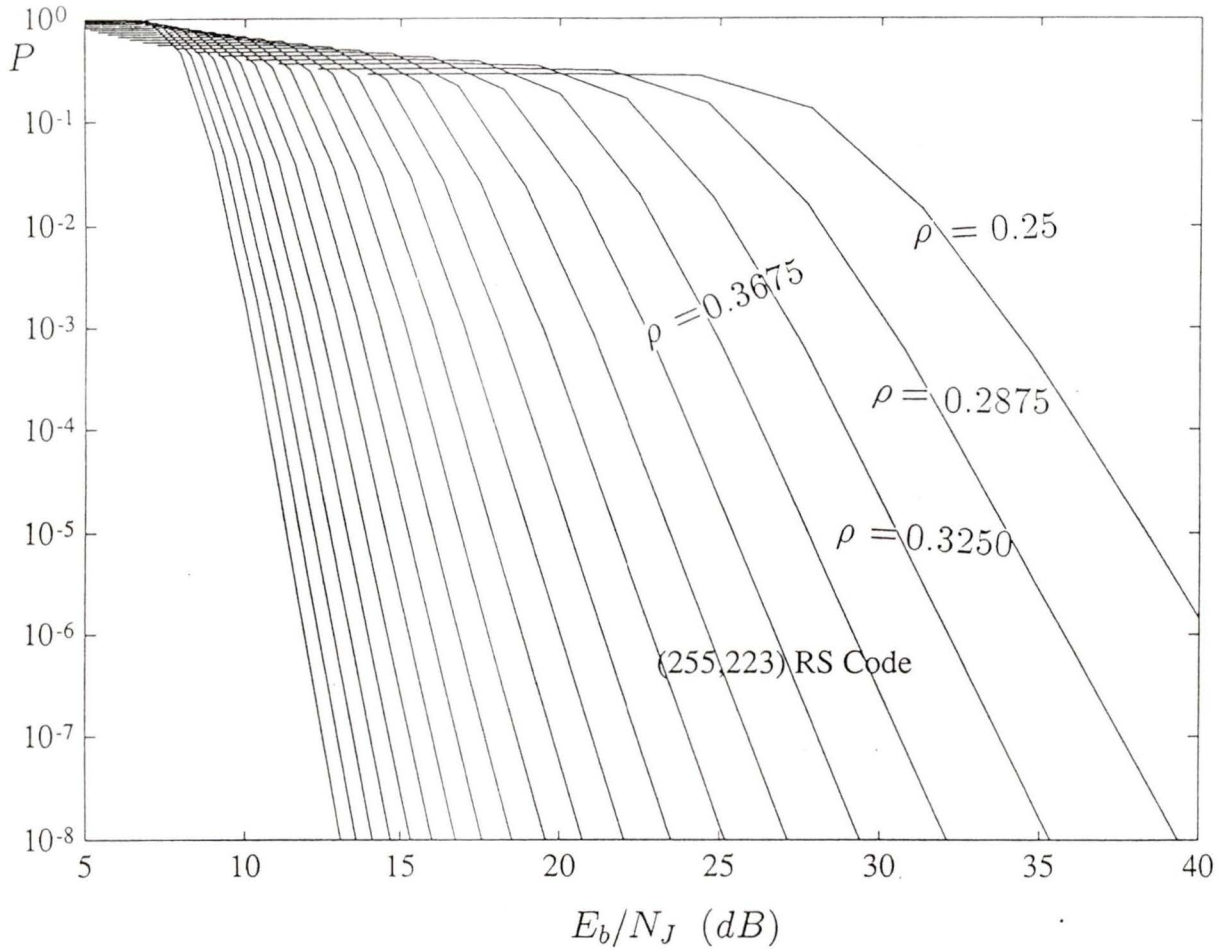


Figure 3.10: The average decoded error probabilities under worst case tone jamming. Ideal interleaving is applied. (255, 223) RS code over $GF(2^8)$ is used to correct up to 16 errors. $SNR = 10dB$.

3.5 Conclusions

In this chapter, the block and decoded error probabilities in the presence of both tone interference and AWGN are studied. The effectiveness of interleaving on the codeword error probability is discussed, and the performance under worst case tone jamming is evaluated when interleaving technique is used.

The results indicate that there exists a code rate at which coding provides optimum performance in the presence of both tone interference and AWGN.

Interleaving can greatly reduce the error probability of the codeword consisting exclusively of '00000000' blocks because it eliminates the strong correlation between the code symbol errors.

Chapter 4

An Application of Universal Receiver Theory to SFH/DPSK with Tone Interference and AWGN

4.1 Introduction

In this chapter, in trying to find a receiver which can improve the performance of SFH/DPSK in the tone jamming environment and AWGN, a parallel approach to the design of a universal receiver for channels with changing characteristics is introduced. The application of this approach to SFH/DPSK systems with tone jamming and AWGN is presented.

In the last two chapters, the performance of coded SFH/DPSK relative to various interference was analyzed. One assumption which is implicit in the analysis is that the structure of equal decision regions [11] is employed by the DPSK demodulator. In fact, this detection scheme is optimum only when the interference is a completely uncorrelated random process like AWGN. For tone interference, whose statistical characteristics are quite different from AWGN, each channel with specific parameters

has its corresponding structure of decision regions that provides minimal decision error probability. We call each of these structures an *optimal decision region* for the channel. A receiver employing the optimal decision region for a given channel is referred to as an *optimal receiver* for this channel.

In SFH/DPSK systems where the interference includes both tone jamming and AWGN, the optimal decision region varies with the channel parameters, which are usually time-varying or unknown. Thus, it is impractical to design a receiver which always provides optimal demodulation of the channel output. This chapter presents a parallel approach to the design of a universal receiver for SFH/DPSK systems with combined tone interference and AWGN. The goal is to select a finite number of receivers with the property that, for any channel parameters from the set of interest, at least one of the receivers performs almost as well as the optimal receiver. This set of receivers is termed a *universal design*, for it is proposed to place these receivers in parallel to implement universal reception.

In Section 2. we will give a brief description of the general design approach. The system model, problem formulation and a concrete design procedure are presented in Section 3. Some comments are made in Section 4.

4.2 Description of the Design Approach

In classical communications theory, it is usually assumed that the characteristics of the physical channel are known to the transmitter and the receiver. It is also assumed that the receiver knows, or can easily learn, all the parameters of the transmitted signal required to demodulate a signal that is sent over the channel. These assumptions are not valid for unknown or time-varying channels, where not

only does the statistical characterization of the physical channel often change with time, but the receiver may not even know all the parameters of the transmitted signal. The receiver is faced with the task of demodulating the output of a channel with unknown characteristics when the input is a signal with unknown parameters. A systematic approach to the design of a universal receiver for this kind of ‘uncertain channels’ were given in [12]. In this section, we briefly describe the basic ideas underlying the design approach, skipping the mathematical details [12].

From the receiver’s point of view, it makes no difference whether the uncertainty comes from the transmitted signal or the physical channel. For simplicity it is preferable to group the transmitter and the physical channel together and refer to the combination as the *channel*. The channel over which the communication system operates at a given time is called the *channel in effect*. Any *channel in effect* is a member of a set of channels called the *channel class*. The subsystem that performs the demodulation process is called the *receiver*. The goal of a *universal receiver* is to provide nearly optimal demodulation regardless of the channel that is actually in effect.

The implementation of the universal receiver proposed in [12] is based on a parallel configuration of receivers, as depicted in Figure 4.1. This system consists of a finite number of receivers with the property that, for each channel in the channel class, the performance of at least one of the receivers will deviate from the optimal performance for that channel by no more than some prescribed amount. The coding scheme is assumed to generate the intrinsic side information that can be used to determine the best receiver for the channel that is in effect. A possible implementation of a decoding system for this parallel configuration is as follows. For each transmitted codeword, the received codewords at the output of the N parallel receivers are

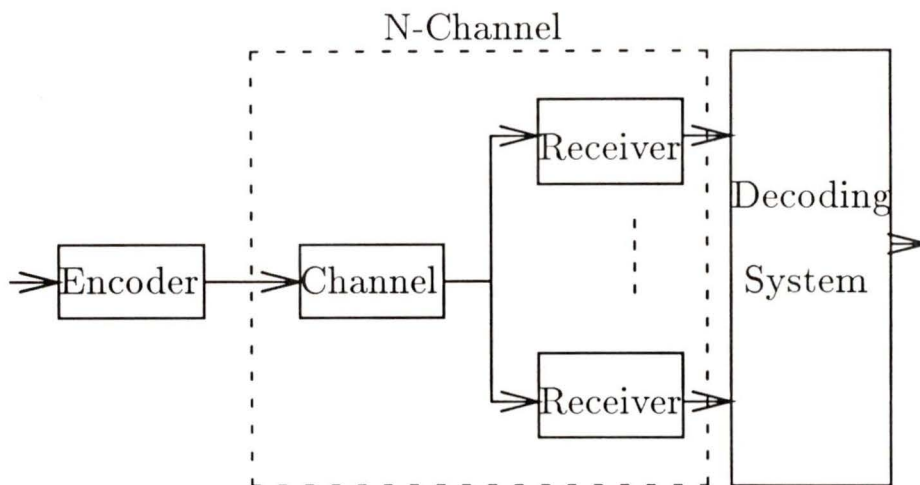


Figure 4.1: A parallel receiver scheme

decoded separately. The output of a good receiver will be correctly decoded with a high probability while the outputs of mismatched receivers will most likely lead to a decoding failure. Reed-Solomon codes may be a good choice for this application because when the free distance of the code is large, the decoding error probability is very small with bounded-distance decoding [13].

Sufficient conditions for the existence of such a universal design are given in [12] by Madhoo. The basic requirements are compactness of the channel class and continuity of the performance function. Madhoo has also pointed out that even if these sufficient conditions are not completely satisfied, it is still possible to carry out a universal design by exploiting specific features of the problem. We illustrate Madhoo's design procedure for two cases where the compactness and continuity requirements are satisfied. The underlying mathematical details can be found in [12].

Let C be the class of channels and R the class of receivers. A *performance*

function $f : C \times R \rightarrow [0, \infty)$ gives the value $f(x, y)$ of the performance measure when receiver y is used and channel x is in effect. We assume that smaller values of $f(x, y)$ correspond to better performance, in conformity with common performance measures such as error probability. Define $g : C \rightarrow [0, \infty)$ by

$$g(x) = \min_{y \in R} f(x, y). \quad (4.1)$$

The value of $g(x)$ is the best possible performance for receivers in R while channel x is in effect. Eq. (4.1) implies that for each $x_0 \in C$, there exists an optimal $y_0 \in R$ such that $g(x_0) = f(x_0, y_0)$.

The allowed deviation from optimality is specified by a continuous function $h : [0, \infty) \rightarrow [0, \infty)$ which satisfies $h(s) > s$ for all $s \in [0, \infty)$. We refer to any such function as a *degradation function*. Given any channel $x \in C$, it is necessary to attain a performance of at most $h[g(x)]$. The form of the degradation function depends on the specific performance characteristics. For instance, if the performance characteristic of greatest interest is error probability, and if error probabilities of less than 10^{-6} are considered satisfactory at the demodulator output, a reasonable choice for the degradation function is $h(s) = \max[p_{min}, ks]$, $s \in [0, 1]$, where a typical value of p_{min} is 10^{-6} . The effect of different choices of p_{min} and k on the design results is demonstrated in the next section.

As stated earlier, the goal of a universal design is to find a finite number of receivers y_1, \dots, y_N in R such that for any given x in C ,

$$\min_{1 \leq i \leq N} f(x, y_i) \leq h[g(x)]. \quad (4.2)$$

Design procedures will be developed for two situations: (a) The channel class

C is a compact subset of a finite-dimensional normed linear space (NLS), and the family of performance functions $\{f(x, y), y \in R\}$ is equicontinuous on C . (b) The channel class C is compact Hausdorff, the receiver class R is a compact subset of a finite-dimensional NLS, and the performance function f is jointly continuous on $C \times R$. The conditions in (a) and (b) are stronger than the sufficient conditions requested for the existence of a universal design. This makes it possible to give constructive procedures for finding a finite number of receivers satisfying Eq. (4.2).

Considering situation (a), we define R_x to be the set of optimal receivers for channel x :

$$R_x = \{y \in R : f(x, y) = g(x)\}. \quad (4.3)$$

Define, for $x \in C$,

$$m(x) = \sup\{r > 0 : \text{For all } u \in B(x, r), f(u, y) \leq h[g(u)] \text{ for all } y \in R_x\}, \quad (4.4)$$

where $B(x, r)$ is the ball of radius r centered at x , and function \sup returns the least upper bound of the set. Let $\delta_C = \inf_{x \in C} m(x)$, where function \inf means the greatest lower bound of the set. If the conditions in (a) situation are satisfied, δ_C is positive. The channel class C can then be partitioned to obtain receivers y_1, \dots, y_N satisfying Eq. (4.2). Considering the one-dimensional example where C is the finite closed interval $[a, b]$, the set of receivers can be chosen by means of the following algorithm.

1. Set $x_1 = a, i = 1$.
2. Choose $y_i \in R_{x_i}$ (That is, choose a receiver that is optimal for x_i).
3. If $x_i + m(x_i) > b$, stop. If not, set $x_{i+1} = x_i + m(x_i)$, increase i by one, and go

to step 2. (The chosen receiver y_i works within the specified degradation for all channels in the interval $[x_i, x_{i+1}]$.)

This procedure terminates in at most $\delta_C^{-1}(b - a)$ steps. The algorithm can be easily modified for channel classes of any finite dimensions.

We now consider situation in (b). Define C_y to be the set of channels for which receiver y is optimal:

$$C_y = \{x \in C : f(x, y) = g(x)\}. \quad (4.5)$$

Let

$$n(y) = \sup\{r > 0 : \text{For all } v \in B(y, r), f(x, y) \leq h[g(x)] \text{ for all } x \in C_v\}, \quad (4.6)$$

where $B(y, r)$ is the ball of radius r centered at y . Let $\delta_R = \inf_{y \in R} n(y)$. δ_R is positive provided conditions (b) are satisfied. The receiver class R can then be partitioned to obtain y_1, \dots, y_N satisfying Eq. (4.2) by means of the following algorithm. Again we formulate it for the one-dimensional example where R is the finite closed interval $[c, d]$.

1. set $y_1 = c, i = 1$.
2. If $y_i + n(y_i) > d$, stop. If not, set $y_{i+1} = y_i + n(y_i)$, increase i by one, and repeat step 2. (The receiver y_i works within the specified degradation for all channels for which any receiver in the interval $[y_i, y_{i+1}]$ is optimal).

This procedure terminates in at most $\delta_R^{-1}(d - c)$ steps, and it can also be modified to handle receiver classes of higher dimensions.

This introduction provides the theoretical framework for carrying out a universal design for channels with changing parameters. In the next section, we apply this theory to the design of a universal receiver for SFH/DPSK systems in the presence of tone interference and AWGN.

4.3 Parallel Receivers for SFH/DPSK with Tone Jamming and AWGN

The problem considered in this section is the design of a universal receiver for a SFH/DPSK system operating under both tone interference and AWGN. The performance of concern is the decision error probability. Binary signaling is assumed with ‘0’ and ‘1’ transmitted with equal probability. Symbols ‘0’ and ‘1’ are represented by the differential phases 0 and π . respectively.

As discussed in the previous chapter, one method of dealing with simultaneous tone interference and AWGN is to add white Gaussian noise to signal vectors which have already been perturbed by a jamming tone with fixed initial phase. The result is then averaged over the pdf of the jamming tone initial phase, which is assumed to be uniformly distributed on the interval $[-\pi, \pi)$.

For ease of reading, the probability for the correct reception of the i th decision conditioned on the signal vectors being jammed is rewritten as follows.

$$p_{ci|\theta_J} = p_r(\phi_1 \leq \phi \leq \phi_2|\theta_J) = \begin{cases} F(\phi_2) - F(\phi_1) + 1 & \phi_1 \leq \Delta\Phi_J \leq \phi_2 \\ F(\phi_2) - F(\phi_1) & \phi_1 > \Delta\Phi_J \text{ or } \phi_2 < \Delta\Phi_J \end{cases} \quad (4.7)$$

where

$$F(\phi) = \frac{W \sin(\Delta\Phi_J - \phi)}{4\pi} \int_{-\pi/2}^{\pi/2} \frac{e^{-G}}{G} dt,$$

and

$$G = U - V \sin t - W \cos(\Delta\Phi_J - \phi) \cos t.$$

The constants U, V and W are

$$U = 0.5(\sigma^{(i)} + \sigma^{(i-1)}),$$

$$V = 0.5(\sigma^{(i)} - \sigma^{(i-1)}),$$

$$W = \sqrt{U^2 - V^2},$$

where

$$\sigma^{(i)^2} = \frac{|A_J^{(i)}|^2}{2N_0}.$$

The difinitions of all notations are as defined in Eq. (3.6).

The probability p_{ci}^J for the i th decision to be correct in both tone jamming and AWGN is therefore

$$p_{ci}^J = \int_{-\pi}^{\pi} p_{ci|\theta_J} \times \frac{1}{2\pi} d\theta_J.$$

In the absence of tone interference, the probability p_{ci}^N for one decision to be correct can be easily obtained from Eq. (4.7) by removing the effect of tone jamming on the signal vectors. By replacing $\Delta\phi_J$ by $\Delta\phi$, which is the differential phase between two consecutively transmitted signal vectors, and $A_J^{(i)}$ by $A^{(i)}$, which is the actual amplitude of the transmitted signal vector, we obtain p_{ci}^N , which is the probability for making a correct decision in AWGN only.

In the binary case, the decision regions are chosen to be symmetric with respect to the X axis, i.e., $\phi_2 = -\phi_1 = \phi_d \in [0, \pi]$. When the phase difference ϕ between

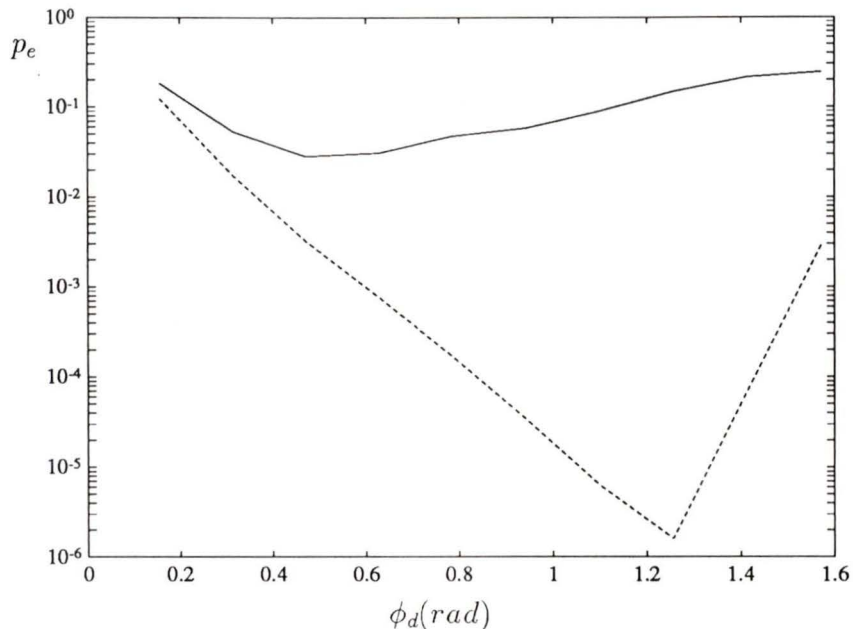


Figure 4.2: The effect of ϕ_d on p_e . For dashed line, $SNR = 35dB$, $SJR = 5dB$, and $\rho = 0.5$. For solid line, $SNR = 20dB$, $SJR = 5dB$, and $\rho = 0.5$.

two received signal vectors lies in $[-\phi_d, \phi_d]$, we decide that symbol ‘0’ is transmitted; otherwise we decide that symbol ‘1’ is transmitted. For certain values of ϕ_d , the error probabilities for symbols ‘0’ and ‘1’ can be obtained by subtracting p_{ci}^J and p_{ci}^N from 1. Let $p_e^J(0|1)$ and $p_e^J(1|0)$ be the error probabilities for symbol ‘1’ and symbol ‘0’ in combined tone interference and AWGN, and $p_e^N(0|1)$ and $p_e^N(1|0)$ be the error probabilities for symbols ‘1’ and ‘0’ in AWGN only. The overall decision error probability p_e is given by

$$p_e = 0.5\rho[p_e^J(0|1) + p_e^J(1|0)] + 0.5(1 - \rho)[p_e^N(0|1) + p_e^N(1|0)]. \quad (4.8)$$

where ρ is the probability for a decision to be jammed.

Figure 4.2 displays the effect of the decision parameter ϕ_d on the performance p_e . It is seen that there exists an optimal ϕ_d^* at which p_e achieves its minimum.

The value of ϕ_d^* varies with the values of SNR , SJR , and ρ . When white AWGN dominates the tone jamming, ϕ_d^* shifts towards $\pi/2$; When tone jamming dominates, ϕ_d^* shifts towards 0. In other words, a receiver is identified by its decision parameter ϕ_d , and the optimal receiver for the channel in effect is determined by the triple of channel parameters (SNR, SJR, ρ) .

Theoretically, both SNR and SJR can range from $-\infty$ to ∞ , violating the compactness condition on the channel class. However, the ranges of SNR and SJR are practically limited by performance requirements.

The channel class of interest is characterized by the set of parameters

$$C = \{(SNR, SJR, \rho) : SNR_{min} \leq SNR \leq SNR_{max}, \\ SJR_{min} \leq SJR \leq SJR_{max}, 0 \leq \rho \leq 1\}. \quad (4.9)$$

Note that C is a compact set in Euclidean 3-space.

The class of available receivers is defined to be

$$R = \{\phi_d : 0 \leq \phi_d \leq \pi\}, \quad (4.10)$$

The performance measure of interest here is the decision error probability at the output of the demodulator. Typically, there is some value of the decision error probability $p_{min} > 0$ such that error probabilities lower than p_{min} are considered sufficient to satisfy the design requirements. Therefore, we are only interested in error probabilities higher than p_{min} in the universal design.

Define $p^*(c)$ as the optimal performance for channel $c \in C$. The universal design problem can be stated as follows: find a finite set of nonnegative real numbers $\{\phi_{d1}, \phi_{d2}, \dots, \phi_{dN}\}$ such that, given any $c \in C$,

$$\min_{1 \leq i \leq N} p(c, \phi_{di}) \leq \max\{p_{min}, h(p^*(c))\}, \quad (4.11)$$

where $p(c, \phi_{di})$ is the error probability when channel c is in effect and receiver ϕ_{di} is used, and h is a degradation function defined on the interval $[0,1]$. An example of such a degradation function is

$$h(x) = kx, \quad x \in [0, 1], \quad (4.12)$$

where $k > 1$ is a design parameter. This particular function allows a multiplicative degradation from the optimal error probability. This form of degradation function with various choices of k is adopted in our numerical evaluation.

It is clear that C and R are both compact, and the performance function p is continuous over $C \times R$. Either algorithm for situation (a) and (b) is applicable here. Since the receiver class is one dimensional but the channel class is three dimensional, it is easier to implement the design by partitioning the receiver class, i.e., using the second algorithm.

The design procedure consists of three major steps:

- 1) Find the set of optimal receivers R^* so that for each $c \in C$, there is a $\phi_d \in R^*$ which provides a minimal error probability $p^*(c)$.

This step is carried out by minimizing Eq. (4.8) with regard to every triple $(SNR, SJR, \rho) \in C$.

- 2) Find $C^*(\phi_d)$ for each $\phi_d \in R^*$, where $C^*(\phi_d) \subset C$ is the subset of channels for which ϕ_d is the optimal receiver.

Define , for any $\phi_d \in R^*$,

$$n(\phi_d) = \sup\{u > 0 : \text{For all } \phi'_d \in [\phi_d, \phi_d + u], \\ p(c, \phi_d) \leq \max[p_{min}, h(p^*(c))] \text{ for all } c \in C^*(\phi'_d)\}. \quad (4.13)$$

Thus, if $\phi_d \leq \phi'_d \leq \phi_d + n(\phi_d)$, then the receiver ϕ_d is nearly optimal for all channels for which ϕ'_d is optimal. The computation of the function n involves a fairly complicated optimization. Once $n(\phi_d)$ is obtained for all $\phi_d \in R^*$, the third step is

- 3) Partition the set of optimal receivers R^* to obtain a finite number of receivers with the property that at least one of them provides a performance which is within the specified degradation from the optimality no matter which channel is in effect.

The last step of partitioning can be done in the following substeps

1. Set $i=1$, $\phi_{d1} = \inf\{\phi_d, \phi_d \in R^*\}$.
2. If $\phi_{di} + n(\phi_{di}) > \sup\{\phi_d, \phi_d \in R^*\}$, stop. If not, set $\phi_{d(i+1)} = \phi_{di} + n(\phi_{di})$, increase i by one, and repeat step 2.

A single channel class is considered for implementation. The receiver design procedure is carried out for several choices of the degradation function. The channel class is chosen as

$$C = \{(SNR, SJR, \rho) : 15 < SNR < 25, 10 < SJR < 20, 0 < \rho < 1\}, \quad (4.14)$$

and the resultant designs are presented in Table 4.1.

It is evident from the results that the less the required degradation from optimality, the more receivers are to be used. Users can decide on the number and the placement of the receivers according to their own performance requirements.

Degradation function, $h(x)$	Placement of receivers, $\phi_d(rad)$	Number of Receivers
$\max(10^{-3}, 10x)$	1.06288, 1.45001	2
$\max(10^{-4}, 5x)$	1.06288, 1.31978	2
$\max(10^{-5}, 3x)$	1.06288, 1.28602, 1.45621	3
$\max(10^{-6}, 1.5x)$	1.06288, 1.20541, 1.30932, 1.46696	4

Table 4.1: Some typical designs for SFH/DPSK systems with tone jamming and AWGN. $SNR \in [15, 25]$, $SJR \in [10, 20]$, $\rho \in [0, 1]$.

4.4 Comments

It has been shown that the parallel approach to the design of a universal receiver has its application in SFH/DPSK systems with tone jamming interference and AWGN. The system performance is improved by employing the designed receiver. However, there is a tradeoff between the number of receivers and the allowed degradation from optimality.

The identification of the best receiver component for the channel in effect is expected to be achieved by making use of the side information provided by certain type of coding schemes, such as Reed-Solomon codes. The design and performance analysis of such a system calls for future work.

Chapter 5

Summary and Future Work

5.1 Summary

This thesis undertook the work of analyzing and improving the performance of coded SFH/DPSK in jamming environment and AWGN. The types of interference considered were AWGN, PBN and tone jamming which are commonly encountered in SFH/DPSK systems. Block and decoded error probabilities were derived and computed with the error correlation in DPSK demodulation considered. The effectiveness of interleaving technique was studied. The error probabilities under worst case jamming were presented.

To deal with the uncertainty of channel characteristics caused by the changing jamming strategies, a parallel approach for designing a universal receiver was introduced and applied to SFH/DPSK systems to improve the performance in tone interference and AWGN. Some typical designs which can provide nearly optimal performance were demonstrated.

5.2 Suggestions for Future Work

Some topics are now of interest concerning the anti-jam capability of SFH/DPSK systems [14].

In conventional DPSK modulation, the information is carried by only one differential phase. Recently, a generalized DPSK scheme was proposed in which the information is differentially encoded in several differential phases. One advantage of this scheme is that by doing multi-symbol detection, the modulation carrier can be estimated over a multi-symbol observation window. The other is that the arithmetic code in the differential phases of multiple symbols can provide some protection against the interference. This multi-symbol DPSK can also be used with SFH, and much work is required to find the anti-jam performance of such SFH/DPSK system.

Another topic that appears to be interesting is intelligent anti-jam receiver. The classical anti-jam strategy is based on the assumption that the jammer knows everything about the receiver and communication system parameters. All the communicator can do is to choose a system that can provide acceptable performance even under the worst case jamming. The idea of an intelligent anti-jam receiver is to change the passive role of the communicator. Certain features can be built into the communication system based on the game theory to improve its anti-jam performance. It requires future work to study the practical strategies that can be implemented in the anti-jam communications, and the performance gain that can be obtained.

Bibliography

- [1] J. G. Proakis, *Digital Communications*. New York: McGraw-Hill, pp. 265-272, 1989.
- [2] J. Salz and B. R. Saltzberg, "Double error rates in differentially coherent phase systems," *IEEE Trans. Commun. Syst.*, Vol. COM-12, pp. 202-205, June, 1964.
- [3] J. F. Oberst and D. L. Schilling, "Double error probability in differential PSK," *Proc. IEEE*, Vol. 56, pp. 1099-1100, June, 1968.
- [4] J. Goldman, "Multiple error performance of PSK systems with cochannel interference and noise," *IEEE Trans. Commun. Technol.*, Vol. COM-19, pp. 420-430, Aug., 1971.
- [5] M. K. Simon, J. K. Omura, R. A. Scholtz, and B. K. Levitt, *Spread Spectrum Communications*, Vol. II, Rockville: Computer Science Press, pp. 73-91, 1985.
- [6] G. Boudreau and R. J. Keightley, "FASSET: A development model for a Canadian EHF MILSATCOM system," *Proc. Canadian Conference of Electrical and Computer Engineering*, Ottawa, Ontario, Canada, Sept., 1990, pp 28.5.1-28.5.4.
- [7] R. F. Pawula, S. O. Rice and J. H. Roberts, "Distribution of the phase angle

- between two vectors perturbed by Gaussian noise," *IEEE Trans. Commun.*, Vol. COM-30, pp. 1828-1841, Aug., 1982.
- [8] S. Lin and D. J. Costello, Jr., *Error Control Coding: Fundamentals and Applications*. Englewood Cliffs, NJ: Prentice Hall, pp. 170-177, 1983.
- [9] E.N. Gilbert, "Capacity of a burst-noise channel," *BSTJ*, Sept., 1960.
- [10] Qiang Wang, T. Aaron Gulliver, and Vijay K. Bhargava, "Probability Distribution of DPSK in Tone Interference and Applications to SFH/DPSK," *IEEE Jour. on Selected Areas in Commun.* Vol. 8, No. 5, pp. 895-906, June, 1990.
- [11] Q. Wang, G. Li, I.F. Blake, V.K. Bhargava, Q. Chen and T.A. Gulliver, "Coding for Frequency Hopped Spread Spectrum Satellite Communications," *Annual Report to Communications Canada under SSC Contract No. 36001-0-3503/01-SS*, pp. 123-145, March, 1991.
- [12] Upamanyu Madhow, "A Parallel Systems Approach to Universal Receivers," *Ph.D. Dissertation, the University of Illinois at Urbana-Champaign*, Aug., 1990.
- [13] Robert J. McEliece and Laif Swanson, "On the Decoder Error Probability for Reed-Solomon Codes," *IEEE Trans. Inform. Theory*, Vol. 32, No.5, pp. 701-703, Sept., 1986.
- [14] Q. Wang, G. Li, I.F. Blake, V.K. Bhargava, and Q. Chen, "Coding for Frequency Hopped Spread Spectrum Satellite Communications," *Annual Report to Communications Canada under SSC Contract No. 36001-0-3503/01-SS*, pp. 65-87, March, 1992.

VITA

Surname: Chen

Given Names: Qingxin

Place of Birth: Quanzhou, China

Date of Birth: December 17, 1966

Educational Institutions Attended:

Southeast University, China

1985 to 1989

University of Victoria, Canada

1990 to 1992

Degrees Awarded:

B.Eng.

Southeast University, China

1989

Publications:

- 1) Qiang Wang and Qingxin Chen, "Block and decoded error probabilities of DPSK in AWGN", presented at *The Twenty-fifth Annual Conference on Information Sciences and Systems*, Baltimore, MD, U.S.A., March, 1991, in the Conference Proceedings, pp 395 - 401.
- 2) Qiang Wang, Qingxin Chen, V. K. Bhargava, and L.J. Mason "Block and decoded error probabilities of DPSK in AWGN", to be published in *IEEE Trans. Commun.*
- 3) Qingxin Chen, Qiang Wang, and V. K. Bhargava "Error performance of coded SFH/DPSK in AWGN and tone interference", to be presented at *IEEE Mil-Com '92*, San Diego, California, U.S.A., October 11-14, 1992.

PARTIAL COPYRIGHT LICENSE

I hereby grant the right to lend my thesis to users of the University of Victoria Library, and to make single copies only for such users or in response to a request from the Library of any other university, or similar institution, on its behalf or for one of its users. I further agree that permission for extensive copying of this thesis for scholarly purposes may be granted by me or a member of the University designated by me. It is understood that copying of this thesis for financial gain shall not be allowed without my written permission.

Title of Thesis :

PERFORMANCE ANALYSIS AND IMPROVEMENT OF SFH/DPSK IN JAMMING INTERFERENCE AND AWGN

Author: _____

Qingxin Chen

September 1, 1992